ARTICLE

Microbial symbionts regulate the primary Ig repertoire

Yuezhou Chen[1], Neha Chaudhary[1], Nicole Yang[1] ID, Alessandra Granato[1], Jacob A. Turner[1], Shannon L. Howard[1], Colby Devereaux[1], Teng Zuo[1], Akritee Shrestha[1], Rishi R. Goel[1], Donna Neuberg[2], and Duane R. Wesemann[1] ID

The ability of immunoglobulin (Ig) to recognize pathogens is critical for optimal immune fitness. Early events that shape preimmune Ig repertoires, expressed on IgM+ IgD+ B cells as B cell receptors (BCRs), are poorly defined. Here, we studied germ-free mice and conventionalized littermates to explore the hypothesis that symbiotic microbes help shape the preimmune Ig repertoire. Ig-binding assays showed that exposure to conventional microbial symbionts enriched frequencies of antibacterial IgM+ IgD+ B cells in intestine and spleen. This enrichment affected follicular B cells, involving a diverse set of Ig-variable region gene segments, and was T cell–independent. Functionally, enrichment of microbe reactivity primed basal levels of small intestinal T cell–independent, symbiont-reactive IgA and enhanced systemic IgG responses to bacterial immunization. These results demonstrate that microbial symbionts influence host immunity by enriching frequencies of antibacterial specificities within preimmune B cell repertoires and that this may have consequences for mucosal and systemic immunity.

Introduction

The combined effect of Ig diversification and selection generates primary Ig repertoires available for adaptive immune responses. Primary *Ig* diversification occurs via assembly of *Ig* variable region (*V*) exons of both heavy (IgH) and light (IgL) chains from component V, (D), and J gene segments through V(D)J recombination. The resulting expression of IgM on immature B cell surfaces forms the antigen-binding part of the BCR, which mediates both negative and positive selection of B cells as they mature into subsets that contribute to the primary Ig repertoire. The more innate-like B1 and splenic marginal zone B cells are known to be positively selected toward self-ligands to form restricted, polyreactive BCR repertoires (Arnold et al., 1994; Hayakawa et al., 1999; Dammers et al., 2000; Martin and Kearney, 2000), whereas the role of positive selection of follicular B cells is less well defined.

Antigen-mediated selection can occur as soon as IgM is produced on the B cell surface of immature B cells through BCR editing. BCR editing is thought to largely be a negative selection process resulting from immature BCR engagement of local antigens, which can mediate a suppression of self-reactive and polyreactive specificities from the mature B cell repertoire (Retter and Nemazee, 1998; Halverson et al., 2004). As developing B cells transition from the immature B cell stage into mature naive IgM+ IgD+ B cell stages, less well-defined selection events continue to

influence their preimmune BCR repertoires. Experiments examining B cell maturation in the spleens (SpLs) of BCR transgenic mice have shown that ligand-mediated positive selection is required for entry into the naive B cell pool with the use of model antigen expression (Cyster et al., 1996) or by provision of a BCR cross-linking antibody (Ab; Wang and Clarke, 2003). Positive selection of newly formed B2 cells has also been examined in the setting of natural BCR repertoires. In this regard, comparisons of immature and mature naive Ig repertoires have shown differences in V gene segment usage, including expansion of selected clones, implying that many conventional preimmune B cells have been ligand selected (Gu et al., 1991; Levine et al., 2000). However, the ligands responsible for selection of conventional B cells into the preimmune B cell pool have not been defined.

Based on findings implicating gut luminal content exerting influence on B cell diversification and/or primary BCR selection in young chickens, rabbits, pigs, and lambs (Wesemann, 2015) and the highly dynamic nature of the Ig repertoire in youth (Lindner et al., 2015), we hypothesized that symbiotic microbes may play a role in preimmune B cell selection early in life. To directly examine this, we used assay systems to examine the degree to which preimmune BCR reactivities to microbial symbionts are influenced by exposure to symbiotic microbes and whether this

[1]Department of Medicine, Division of Rheumatology, Immunology, and Allergy, Brigham and Women's Hospital and Harvard Medical School, Boston, MA; [2]Department of Biostatistics and Computational Biology, Dana-Farber Cancer Institute, Boston, MA.

Correspondence to Duane R. Wesemann: dwesemann@bwh.harvard.edu.

may be associated with positive or negative selection. We report that microbial symbionts influence host immunity by delivering forces that enrich preimmune B cell repertoires early in life with antibacterial specificities, impacting both systemic and mucosal immune responses.

Results

Detection of BCR reactivity to SIC

To explore how perturbations in intestinal luminal content may influence the naive B cell Ig repertoire, we used limiting dilution analysis (LDA; Vale et al., 2012) to measure frequencies of intestinal bacteria-reactive Ig isolated from naive B cells from germ-free (GF) mice compared with conventionalized littermate controls. For LDA, B cells are sorted into wells in serial dilutions and stimulated for Ab production. ELISA then determines binding ability of secreted Ab in supernatants to bacteria cultured from intestinal content.

We also designed a method to estimate frequencies of preimmune Ig reactivity to general intestinal content. The bacteria-sized insoluble fraction of specific pathogen-free (SPF) mouse small intestine luminal content (SIC) was fluorescently labeled and used as a B cell stain (Fig. S1 A). The contribution of BCR to cellular SIC-binding was estimated by staining cells with SIC after treatment with an Ab to Igκ or an isotype control Ab. Most B cells express Igκ as a part of their BCR, and treatment with anti-Igκ reduces BCR from the cell surface due to endocytic internalization (Fig. S1, A–C), but does not interfere with SIC interaction with BCR (Fig. S1, E–H). By normalizing the signal loss with BCR internalization to IgM signal loss, we calculate a binding index that reports BCR-dependent binding activity (Fig. S1 D). Control comparisons of the SIC-binding index of B cells from monoclonal BCR knock-in mice to wild type mice indicate the degree of signal likely attributable to BCR recognition (Fig. S1 I). While this cell-binding assay has the advantage of assessing cells directly for BCR-binding ability to a diverse microbiota (Fig. S1 M), the LDA assay described above appeared to be superior in discriminatory power, but reports binding only to culturable microbiota isolated from mouse intestine, which is largely *Lactobacillus* and Enterobacteriaceae (Fig. S1 M). We therefore use both assays to examine our hypothesis.

Microbial symbionts enrich naive B cell repertoires with antibacterial specificities

To determine the degree to which microbial symbionts influence the frequency of B cells reactive to SIC in the preimmune Ig repertoire, we performed LDA and SIC-binding index assays of IgM+ IgD+ B cells from weanling Swiss Webster (SW) GF mice to littermates that were conventionalized with SPF microbiota for 21 d starting from weaning age (postnatal day 21). Both groups were analyzed at the age of 42 d of life. IgM+ IgD+ cells from both SpL and lamina propria (LP) at weaning age are essentially all naive, as indicated by the observation that nearly all splenic and LP B cells are GFP+ in 3-wk old *BAC-Rag2pGFP* mice (Yu et al., 1999), a model where developing B cells fluoresce up to 4 d after completion of IgH and IgL assembly (Fig. S1, J–L; Nagaoka et al., 2000). Most cells remain GFP+ at 42 d of life (Fig. S1, J–L).
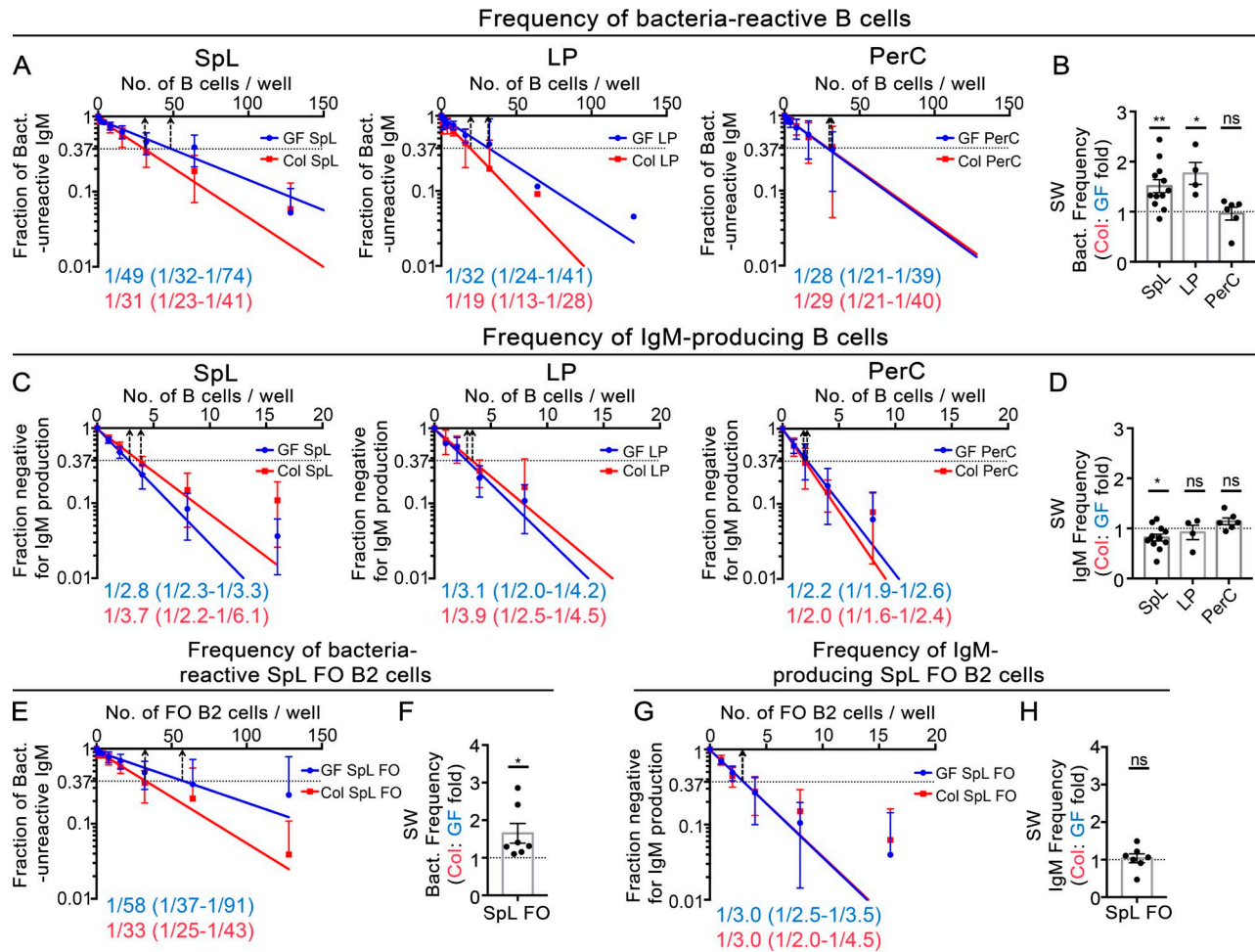
By LDA, a mean of ~1/49 (0.021 ± 0.0068) GF splenic B cells are reactive to cultured intestinal bacteria, and this changes to a mean of 1/31 (0.033 ± 0.0090) in conventionalized littermates (Fig. 1, A and B). LP B cell reactivity in GF mice is 1/31 (0.032 ± 0.0065), which changes to 1/19 (0.052 ± 0.010) in conventionalized littermates (Fig. 1, A and B). The frequency of bacteria-reactive clones in peritoneal cavity (PerC) B cells, which are enriched for B1 cells (Baumgarth, 2010), remained unchanged (Fig. 1, A and B). We also measured total IgM production and found that the increase of bacterial binding frequencies in young colonized mice was not caused by higher frequency of IgM production after in vitro activation of the B cells (Fig. 1, C and D). Statistical analysis normalizing conventionalized samples to paired littermate controls showed over a 50% increase of mean bacterial binding frequencies upon conventionalization in both SpL and LP (Fig. 1 B).

We also performed SIC binding index measurements. With regard to SIC isolated from colonized mice (ColSIC), largely of *Lactobacillus* and *S24-7* (Fig. S1 M), we found that LP and splenic B cells from conventionalized mice demonstrated increased BCR-dependent binding compared with GF littermates (Fig. S2, A, C, and E). Binding index measurements to GFSIC were unchanged between GF and conventionalized groups (Fig. S2, A–E), suggesting that the observed enrichment of luminal reactivity may largely be specific for microbial antigens. These results indicate that exposure to microbial symbionts can result in enrichment toward bacterial reactivity in the primary Ig repertoire.

Follicular B2 cells are responsible for the symbiont-dependent Ig repertoire shift

To explore the role of symbiotic microbes on B cell subset distributions, we compared GF mice to littermates that were conventionalized for 21 d, beginning at early weaning age (postnatal day 21). After 21 d of conventionalization (postnatal day 42), we found that splenic and LP IgM+ IgD+ B cells were present at similar amounts compared with littermates that remained GF (Fig. 2 A). In addition, levels of splenic B1, PerC B1 cells, and conventional B cells with a follicular B cell phenotype were similar in the GF and conventionalized littermate mice (Fig. 2, B–D and F), whereas there was a mild decrease in the frequency of marginal zone B cells (Fig. 2, D and E) and a mild increase in the frequency of progenitor and splenic transitional B cells in conventionalized mice (Fig. 2 G). We didn't find B220loCD93+CD23− B cells that can be convincingly categorized as transitional B cells (B220loCD93+CD23−) in LP B cell preparations (Fig. 2 H).

We deployed LDA and the SIC cell-binding assay to test which B cell compartment/subset is responsible for the increase in bacterial reactivity upon microbial colonization to the young GF SW mice. Compared with GF mice, we found that the ColSIC index increased significantly in follicular B cells, but not splenic B1 (CD93− CD23− CD43+), PerC B1 (CD93− CD23− CD11b+), or marginal zone (MZ; CD93− CD23− CD21+) B cells from conventionalized SW littermates (Fig. S2, F–H). LDA experiments demonstrated a 60% increase of mean bacterial binding frequencies of splenic follicular B cells from 1/58 (0.017 ± 0.0053) to 1/33 (0.031 ± 0.0060) after 21-d conventionalization (Fig. 1, E–H). Analysis of memory B cell subsets using CD80, CD73, and PD-L2 (Anderson et al., 2007;

Chen et al.
Microbial symbionts regulate the primary Ig repertoire

Journal of Experimental Medicine
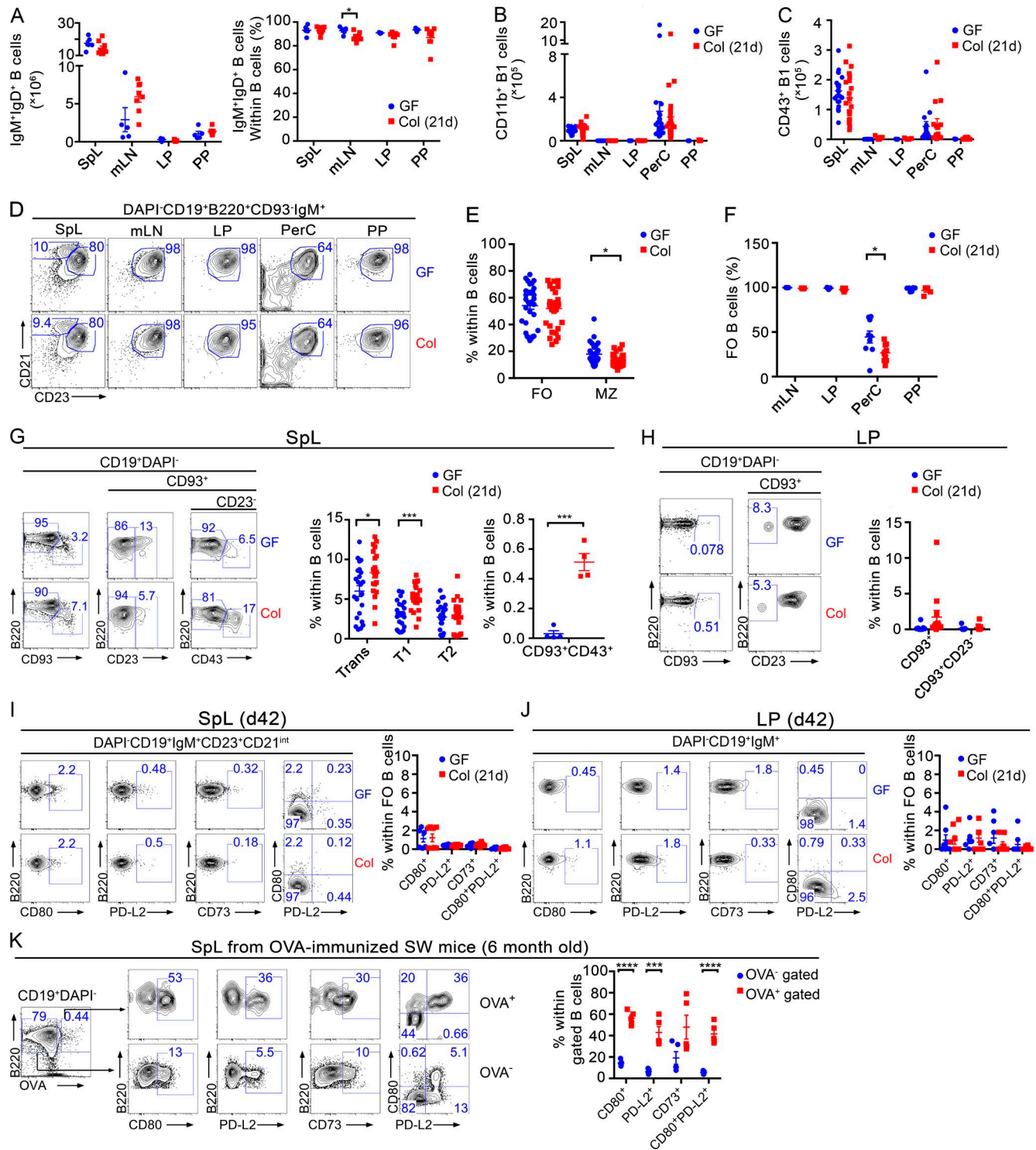https://doi.org/10.1084/jem.20171761

1398

Figure 1. **Exposure of weanling GF mice to microbial symbionts leads to increased bacterial reactivity in the primary Ig repertoire. (A–H)** LDA line graphs (A, C, E, and G) and fold-change bar graphs (B, D, F, and H) showing comparisons of frequencies of bacteria-reactive IgM (A, B, E, and F) and total IgM-producing B cells (C, D, G, and H) of the indicated sorted cells from GF (blue; n = 4–12) or mice colonized with SPF microbiota (Col, red; n = 4–12). Splenic B cells were sorted based on a DAPI⁻ B220⁺. Splenic follicular (FO) B cells were sorted based on the DAPI⁻ B220⁺ CD93⁻ GL7⁻ CD95⁻ CD43⁻ CD23⁺ CD21int phenotype. Dots indicate individual mice. Data are from 4–10 independent experiments. P-values were calculated using the one-sample t test. The dashed line in the bar graphs indicates the null hypothesis. For the LDA, the number of IgM-producing cells giving rise to 37% of wells negative for bacteria binding defines the frequency of reactivity based on Poisson statistics as described (Vale et al., 2012). Numbers in parenthesis in A, C, E, and G indicate 95% confidence intervals (CI). Dotted arrows indicate the minimum number of cells required to recover bacteria-reactive IgM (A and E) or total IgM production (C and G). Error bars indicate ± 95% CI (A, C, E, and G) or ± SEM (B, D, F, and H). *, P < 0.05; **, P < 0.01. ns, not significant. Conventionalization occurred for 21 d beginning at the age of postnatal day 21.

Zuccarino-Catania et al., 2014) showed no measurable difference between GF and colonized littermates from a very low baseline at a young age (day of life 42; Fig. 2 I and J). Memory B cells from OVA-immunized mice were used as a positive control for the memory B cell stains (Fig. 2 K). Together, these results suggest that host exposure to microbial symbionts leads to an enrichment of antibacteria specificities in preimmune follicular B2 cells.

Unswitched B cells occupy a distinct mucosal niche
We performed immunostaining and microscopic analysis of small intestinal tissue sections to determine the localization of B lineage cells in GF and conventionalized SW littermate mice. We found most of the IgA⁺ cells are negative for B220, consistent with a plasma cell phenotype, whereas all the IgD⁺ cells expressed B220. At the age of postnatal day 42, we found the IgD⁺ B220⁺ cells to be distributed throughout the LP and villi,

but with an apparent preference to localize closer to villi bases and, in general, nearer to the serosal surface compared with the IgA⁺ cells (Fig. 3 A, C, D, and F). Localization of B cells with a mature naive phenotype to the serosal surface is reminiscent of the localization of early lineage developing B cells in the weanling-age mice shown previously (Wesemann et al., 2013). IgA⁺ cells outnumbered IgD⁺ B220⁺ cells in conventionalized mice as well as adult SPF mice (Fig. 3, B and E). As expected, the number of LP IgA⁺ cells was greater in conventionalized mice compared with littermates that remained germ free (Fig. 3 B) and in older SPF mice compared with younger SPF mice (Fig. 3 E). There was little to no difference in the number of LP IgD⁺ B220⁺ cells with conventionalization (Fig. 3 B) or aging (Fig. 3 E). Intestinal sections were also evaluated from μMT mice as a negative control as these mice lack peripheral B lineage cells (Kitamura et al., 1991).

Chen et al.
Microbial symbionts regulate the primary Ig repertoire

Journal of Experimental Medicine
https://doi.org/10.1084/jem.20171761

1399

Figure 2. **Composition of B cell subsets in GF and conventionalized littermates. (A)** Dot plots showing numbers and percentages of IgM[+] IgD^{+} B cells from the indicated tissues ofGF (*n* = 3–6) and colonized littermates (Col; *n* = 7–9). Data are from two to three independent experiments. **(B and C)** Dot plots showing the number of PerC B1 cells (DAPI^{−} CD19^{+} B220^{+} IgM^{+} CD93^{−} CD23^{−} CD11b^{+}; B) or splenic B1 cells (DAPI^{−} CD19^{+} B220^{+} IgM^{+} CD93^{−} CD23^{−} CD43^{+}; C) from indicated tissues of young GF (*n* = 9–23) and colonized littermate (Col; *n* = 11–24) mice. Data are from four to six independent experiments. **(D–F)** FACS plots (D) and scatter plots (E and F) showing the percentage of B cells with follicular (FO) B cell (DAPI^{−} CD19^{+} B220^{+} IgM^{+} CD93^{−} CD23^{+} CD21^{int}) and marginal zone (MZ) B cell (DAPI^{−} CD19^{+} B220^{+} IgM^{+} CD93^{−} CD23^{−}CD21^{hi}; D and E) phenotypes from GF (*n* = 5–23) and colonized SW littermates (Col; *n* = 5–21). Data are shown for two to seven independent experiments. **(G)** FACS plots and scatter plots showing the percentage of splenic transitional (Trans) B cells (DAPI^{−} CD19^{+} B220^{low} CD93^{+}), transitional 1 (T1) B cells (DAPI^{−} CD19^{+} B220^{low} CD93^{+} CD23^{−}), transitional 2 (T2) B cells (DAPI^{−} CD19^{+} B220^{low} CD93^{+} CD23^{+}), and progenitor B cells (DAPI^{−} CD19^{+} B220^{low} IgM^{−} CD93^{+} CD43^{+}) from GF (*n* = 4–23) and colonized littermates (Col; *n* = 4–21). Data are shown for 2–10 independent experiments. **(H)** FACS plots and scatter plot showing the percentage of LP B cells with CD93^{+} and CD93^{+} CD23^{−} phenotypes from GF (*n* = 15) and colonized littermates (Col; *n* = 13). Data are shown for five independent experiments. **(I and J)** FACS plots and scatter plots showing the percentage of splenic B cells (I) and LP B cells (J)

Chen et al.
Microbial symbionts regulate the primary Ig repertoire

Journal of Experimental Medicine
https://doi.org/10.1084/jem.20171761

1400

Microbial symbionts influence V_H usage frequencies

We sequenced Ig genes of GF and conventionalized littermates to gain insights into how symbiotic microbes influence Ig repertoires on a global level. We sorted naive splenic follicular B cells and LP B cells from GF mice and littermates that were conventionalized at weaning age for either 7 or 21 d for analysis on day-of-life 28 (for 7 d colonization) or day-of-life 42 (for 21 d colonization). We sequenced Ig genes using B cell cDNA synthesized with unique molecular identifiers (UMIs) to exclude PCR repeats in the analysis (Table S1). We found that the naive Ig repertoire of both GF and colonized mice in general showed similar degrees of clonal complexity and overall V_H gene segment usage preference (Fig. 4, A–C) and clonal expansions (Fig. 5). We also observed a trend toward increased diversity in conventionalized mice (Fig. 4 B). Jensen-Shannon divergence (JSD), which reports overall divergence on a scale of 0 to 1, with 1 being full difference, showed that overall V_H gene segment preference was largely intact between GF and conventionalized samples, with values ranging between 0.03 and 0.1 (Fig. 5, A–F).

To examine potential differences in specific V_H preference caused by the presence of microbial symbionts, we subtracted the frequencies of V_H gene usage of the unique B cell clonotypes in GF mice from that of conventionalized littermates and plotted the values in line graphs we refer to as subtraction plots. We then overlaid subtraction plots from different time points and cell groups and determined strength of correlation to understand the timing and predictability of symbiont-dependent changes in V_H preference (Fig. 6). In addition, we plotted conventional correlation plots to measure correlations in V_H frequency differences between treatment groups. We found that splenic follicular B cell Ig repertoires of mice conventionalized for 7 d showed differences in usage frequencies of several V_H gene segments in both positive and negative directions compared with those of GF littermates. The subtraction plot for the 21 d colonization group (Col) – GF littermates showed a signature that was nearly superimposable with that of the 7 d colonization group (Fig. 6, A and B), with a correlation coefficient (r) of 0.87 (P < 0.0001) for splenic FO B cells and 0.77 (P < 0.0001) for splenic transitional 1 (T1) B cells, indicating 76% and 60% covariation, respectively. In contrast, comparison of Col – GF subtraction signals from the 7- and 21-d colonization groups from LP B cells showed very little linear correlation (r = 0.07; Fig. 6 C). These results demonstrate an increased variability in the LP B cell compartment and suggest that the symbiont-related selection forces differ in the LP compared with the SpL.

Because T1 cells are developmental predecessors to follicular B cells, we examined the degree to which microbe-dependent changes in follicular B cells were already apparent in T1 B cells, which had an overall JSD that was similar to that of follicular B cells (Fig. 5, A–D). We compared day 21 Col – GF subtraction plots for T1 versus follicular B cells and find a strong correlation (r =

0.77, 59% covariance, P < 0.0001; Fig. 6 D). These results suggest that conventionalization with symbiotic microbes can lead to consistent V_H preference changes in splenic follicular B cells via a pattern already present in T1 cells. These data also suggest that these changes largely take place by 7 d of colonization.

To determine the degree to which certain V_H gene segments might be favored in B cells reactive to microbial symbionts, we performed single cell sequencing on 74 bacteria-reactive clones and 102 clones that were not reactive to bacteria. We found a diverse use of V_H gene segments for each, with ∼1/2 (21 in 40) V_H segments shared between the groups and no obvious V_H preference in the bacteria-binding group (χ^2 test, P = 0.77; Fig. 6 E). In addition, the bacteria-binding clones from conventionalized mice did not show increased nucleotide mismatch/mutation levels compared with GF sequences (Fig. 6 F).

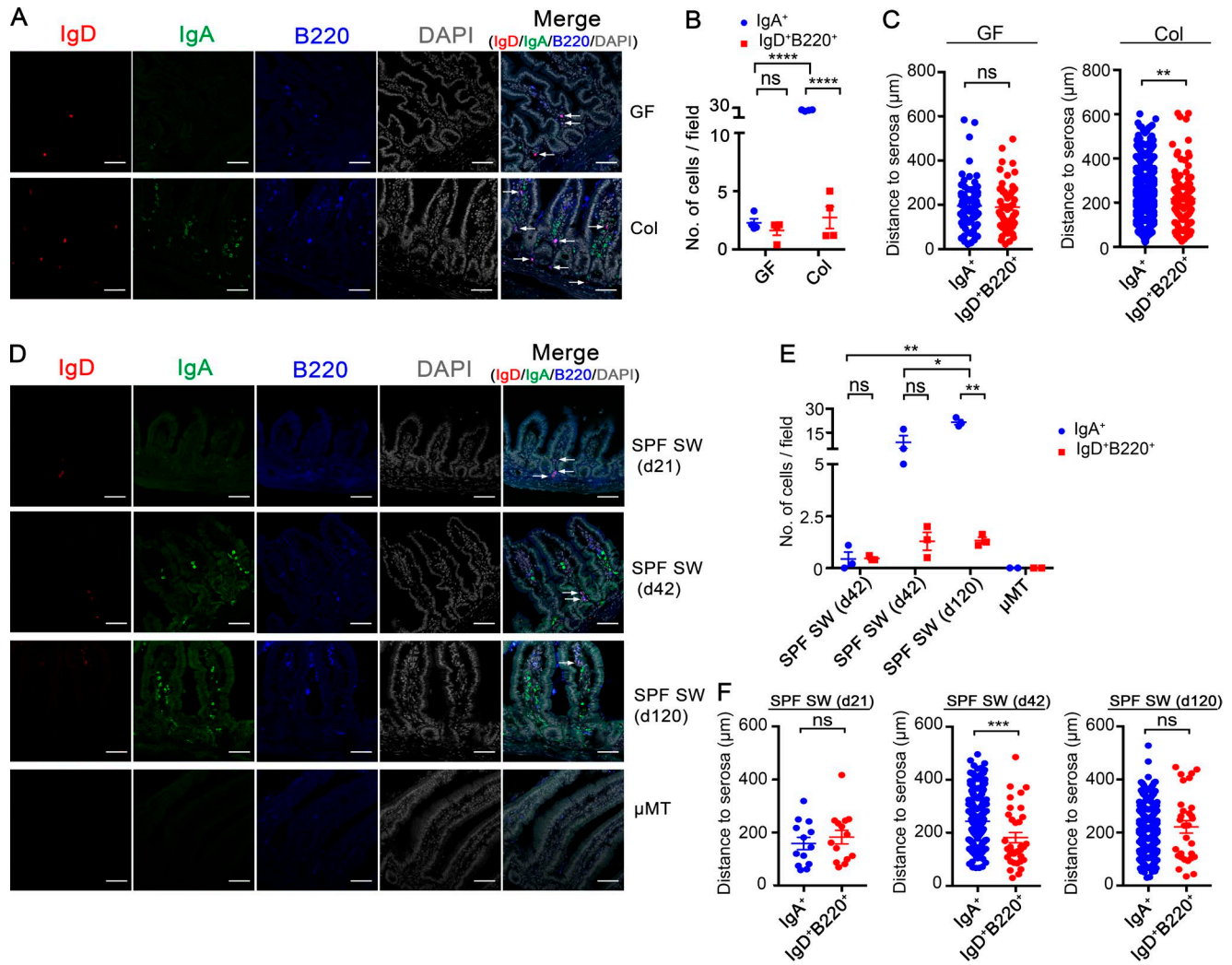## T cell–independent enrichment of antibacterial naive B cells

To examine the role of T cells on microbe-induced enrichment of bacterial reactivity in preimmune repertoires, we depleted the CD4$^+$ T cells in mice during the conventionalization period using a depleting Ab (Fig. 7, A–C; Fig. S3, A–C). CD4$^+$ T cell depletion reduced the level of GL7$^+$ CD95$^+$ GC cells to GF levels (Fig. 7 B; Fig. S3 D). In comparison with the binding index in B cells from GF mice, the ColSIC binding indexes were significantly increased in splenic, LP, and Peyer's patch (PP) B cells in CD4$^+$ cell-depleted colonized mice, to levels as high as isotype Ab-treated conventionalized mice (Fig. S3 E).

We sorted GL7$^-$ CD95$^-$ B220$^+$ B cells from SpL, LP, and PerC of GF, isotype Ab-treated, and CD4$^+$ cell-depleted colonized mice for in vitro activation and assessed the intestinal bacteria-binding activity of secreted Ig by LDA. The bacteria-binding frequencies increased significantly in SpL and LP B cells in both isotype Ab-treated and CD4$^+$ cell-depleted colonized mice (Fig. 7, D–F), whereas their IgM production was similar in all the groups (Fig. 7 G-I). Furthermore, the increase of bacterial binding frequency of splenic follicular B cells after conventionalization of young GF SW mice is independent of CD4$^+$ T cells (Fig. 7, J–O). These results suggest that microbe-mediated regulation of bacteria reactivity in IgM$^+$ IgD$^+$ B cells takes place in a manner that is distinct from selection associated with conventional T cell–dependent immune responses.

IgM$^+$ IgD$^+$ B cells from microbe-experienced mice prime T cell–independent anticommensal IgA

IgA-producing B cells are derived from both innate-like B1 cells, which harbor polyreactive Ig specificities toward molecules expressed by pathogens (Baumgarth, 2010), as well as conventional B2 cells (Pabst, 2012). Mutualistic and commensal bacterial symbionts tend to induce T cell–independent anti-IgA via unknown mechanisms (Macpherson et al., 2000; Bunker et al.,

---

with surface expression of CD80, PD-L2, and CD73 from GF (*n* = 8) and colonized littermates (Col; *n* = 8). Data are shown for two independent experiments. **(K)** FACS plots and scatter plot showing the percentage of splenic B cells with surface expression of CD80, PD-L2, and CD73 gated on OVA$^+$ or OVA$^-$ B cells from OVA-immunized SW mice (*n* = 5). SW mice were immunized with 100 µg OVA in Alum every 3 wk times three, beginning at the age of 2 mo. Spleens were collected 8–9 wk after the last immunization and used as a positive control for the memory marker stains. Data are shown for two independent experiments. Two-tailed *t* test. Error bars in the results indicate ± SEM. *, P < 0.05; ***, P < 0.0005; ****, P < 0.0001. For all the conventionalization experiments, the GF SW littermates were conventionalized to SPF conditions at the age of postnatal day 21 for 21 d.
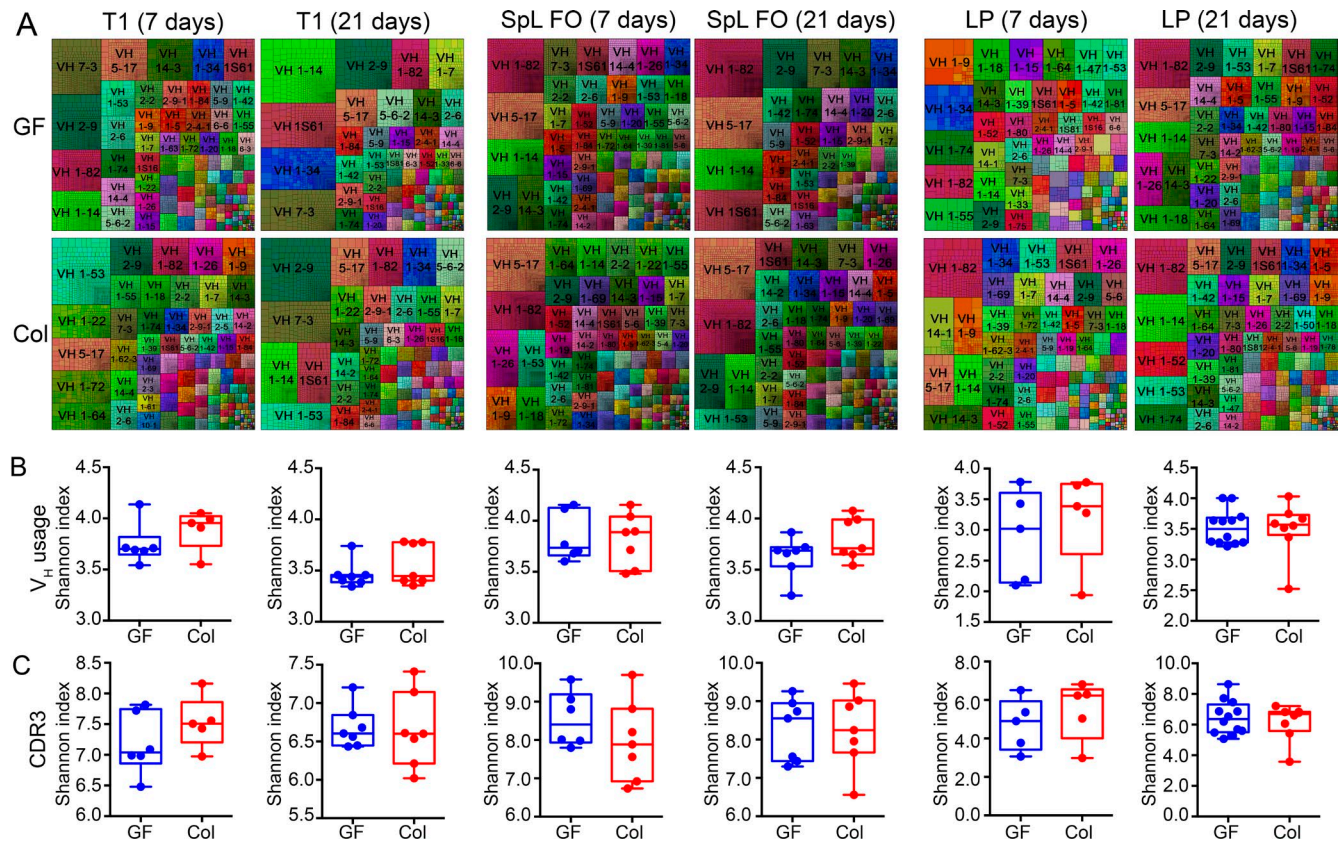
Chen et al.
Microbial symbionts regulate the primary Ig repertoire

Journal of Experimental Medicine
https://doi.org/10.1084/jem.20171761

1401

Figure 3. **Localization of intestinal IgD+ B Cells. (A)** Representative photomicrographs of small intestinal sections stained with DAPI- and fluorophore-conjugated Ab for IgD (FITC), IgA (PE), and B220 (APC) as indicated from GF (*n* = 4) and conventionalized SW littermates (Col, *n* = 4). Photomicrographs shown are representative of one of two independent experiments. **(B)** Dot plot showing the number of LP IgA+ cells and IgD+ B220+ cells per high power field (200×) per GF (*n* = 4; 10 fields/mouse) and conventionalized SW littermates (Col; *n* = 4; 11 fields/mouse) described as in A. **(C)** Dot plots showing the perpendicular distance (see Materials and methods) between individual LP IgA+ cells (*n* = 85 for GF; *n* = 971 for Col), IgD+ B220+ cells (*n* = 59 for GF; *n* = 108 for Col), and the serosal surface from GF (*n* = 4) and colonized SW littermates (Col, *n* = 4) described as in A. **(D)** Representative photomicrographs of small intestinal sections stained as in A from SPF SW mice at the age of postnatal day 21 (*n* = 3), 42 (*n* = 3), and 120 (*n* = 3). Negative control μMT mice (*n* = 2) are also shown. White arrows indicate IgD+ B220+ cells. Bars, 60 μm. Photomicrographs are representative images from one of three independent experiments for each time point and two independent experiments for μMT mice. **(E)** Dot plot showing the number of IgA+ cells and IgD+ B220+ cells per high power field (200×) from SPF SW mice and μMT mice described as in D. **(F)** Dot plots showing the perpendicular distance (see Materials and methods) between individual LP IgA+ cells (*n* = 13 for SPF SW day 21; 10 fields/mouse; *n* = 261 cells for SPF SW day 42, 10 fields/mouse; *n* = 482 cells for SPF SW day 120, 8 fields/mouse), IgD+ B220+ cells (*n* = 14 for SPF SW day 21, 10 fields/mouse; *n* = 34 cells for SPF SW day 42, 10 fields/mouse; *n* = 30 cells for SPF day 120, 8 fields/mouse) and the serosal surface from SPF SW mice described as in D. Two tailed *t* test. Error bars indicate ± SEM. *, P < 0.05; **, P < 0.01; ***, P < 0.0005; ****, P < 0.0001. ns, not significant. GF SW mice were conventionalized by cohousing with SPF mice for 21 d beginning at the age of postnatal day 21.

2015). Toxins, as well as tissue-invasive microbes tend to induce IgA responses through more conventional T cell–dependent mechanisms (Pabst, 2012). Our data described above raise the possibility that selection toward increased commensal reactivity in this context could occur within the preimmune IgM+ IgD+ B cell pool in addition to the selection that likely occurs in the context of activation and maturation to IgA-secreting cells. In this regard, we hypothesized that the increased bacteria reactivity in the primary Ig repertoire from conventionalized mice may prime the production of intestinal bacteria-reactive IgA. To examine

this, we transferred B cells from GF or colonized littermates into *Rag2−/−* mice, which lack mature B and T cells, and measured bacterial reactivity in intestinal lumen IgA (Fig. 8 A). Transfer of splenic B220-selected (Fig. S4, A–C), as well as CD43-depleted (B1 cell–excluded) splenic cells (Fig. S4, D–F) from colonized donor mice to *Rag2−/−* recipients resulted in increased bacteria-reactive luminal IgA in the small intestine, but not in the large intestine (Fig. 8, B and C).

We also excluded B1 and GC cells by flow cytometric sorting of naive splenic B cells of GF and colonized mice (Fig. 8 D; Fig. S4,

Chen et al.
Microbial symbionts regulate the primary Ig repertoire

Journal of Experimental Medicine
https://doi.org/10.1084/jem.20171761

1402

Figure 4. **Clonal complexity and overall V_H gene segment usage in splenic T1 (T1), splenic follicular (FO), and LP B cells of GF versus conventionalized mice. (A)** Tree maps showing the Ig V_H gene segment usage for the sorted splenic transitional 1, splenic follicular, and intestinal LP B cells from GF and littermates cohoused with the SPF mice for 7 or 21 d. Each block represents combined data from all the mice under the same indicated condition (n = 5–12). Unique colors were assigned to each V_H gene segment. The separated individual areas (segments) within each colored box refers to the size of individual clones bearing unique CDR3 regions within the V_H usage pool. The following markers defined T1 cells: DAPI⁻ CD19⁺ B220^low IgM⁺ CD93⁺ CD23⁻; splenic FO B cells: DAPI⁻ CD19⁺ B220⁺ IgM⁺ CD93⁻ CD95⁻ CD43⁻ CD23⁺ CD21^int; and LP B cells: DAPI⁻ CD19⁺ B220⁺ IgM⁺ CD93⁻ CD95⁻ GL7⁻ CD23⁺. **(B and C)** Box plots showing the Shannon diversities of V_H gene segment usage (B) and CDR3 (C) for the sequences shown in A for splenic T1, splenic FO, and LP B cells from GF and colonized (Col) SW littermates. Data are from four and five independent experiments for 7- and 21-d conventionalization experiments, respectively. Conventionalization was initiated at postnatal age day 21.

G–I). The B1- and GC-depleted naive B cells from conventionalized mice produced increased bacteria-reactive IgA in duodenum and ileum of *Rag2*⁻/⁻ mice as compared with GF controls (Fig. 8 E). These results indicate that naive B2 cells from microbe-experienced mice can enrich the bacteria reactivity of small intestinal T cell-independent IgA pools.

IgM⁺ IgD⁺ B cells from symbiont-experienced mice enhance systemic antibacterial immunity

Previous work has shown that symbiotic microbes can have various effects on the immune system to enhance host–microbe homeostasis and health (Hooper et al., 2012). Because we found that exposure to microbial symbionts influenced the preimmune BCR repertoire, we examined the degree to which this repertoire shift of the magnitude seen in our system could be physiologically relevant in the setting of a systemic immune challenge.

We performed adoptive transfer experiments to provide B cell–deficient (μMT) mice with B cells from GF or conventionalized littermates to determine whether commensal microbe-mediated changes in the preimmune B cell repertoire could influence

systemic immunity. Because of the different background strain of μMT mice (C57BL/6J), we first verified that the microbe-dependent changes we observed in SW mice also occur in C57BL/6J mice. In this regard, we found that in colonization of GF C57BL/6J mice resulted in higher antibacterial reactivity in total naive B cell as well as follicular B cells, similar to SW mice (Fig. 9 A-H).

We isolated B cells from GF and commensal microbe-experienced C57BL6/6J mice and transferred them to μMT mice (Fig. 9 I). The transferred B cells were IgM⁺ IgD⁺ and had no detectable differences in B cell follicular and MZ B cell composition (Fig. 9 J). In addition, the amount of GC B cells was low and similar between GF and conventionalized littermates (Fig. 9 J). The mice were then immunized against intestinal bacteria or OVA, and plasma was collected (Fig. 9 I). Upon intestinal bacteria immunization, total levels of IgM and IgG increased with no significant differences between the groups except the latest time point on postimmunization on day 28 (Fig. 9 K and L, right panels). However, when plasma was tested for reactivity to cultured intestinal bacteria, μMT mice that received B cells from conventionalized mice responded with significantly increased antibacterial IgM and IgG at nearly all time points tested, including
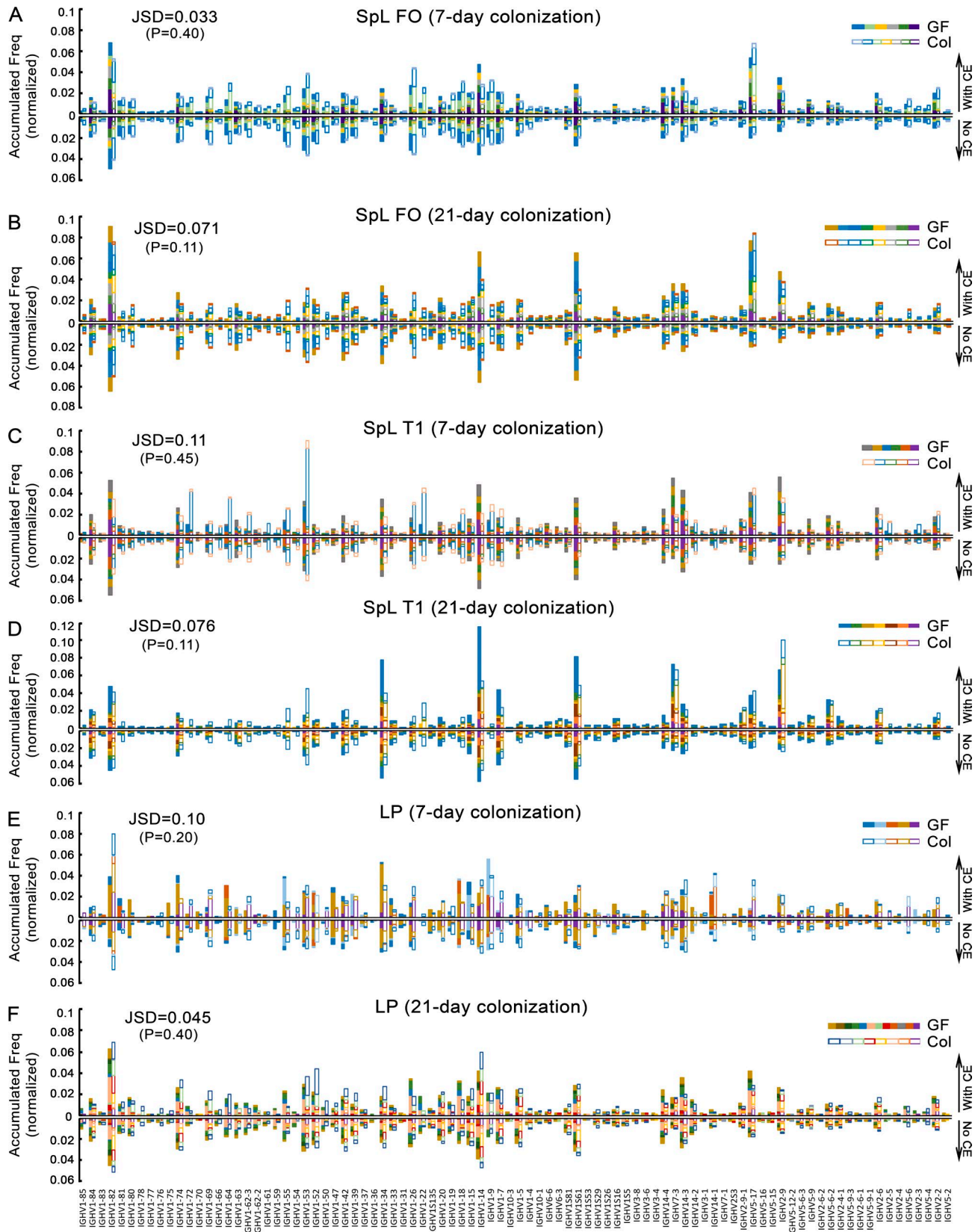
Figure 5. **Normalized accumulated V_H gene segment frequencies in splenic T1, splenic follicular (FO), and LP B cells of GF versus conventionalized mice. (A–F)** Bar graphs showing normalized accumulated frequencies of V_H gene segment usage in sorted splenic follicular (A and B), splenic T1 (C and D), and intestinal LP (E and F) B cells of GF (solid bars; n = 5–12) versus conventionalized (open bars; n = 5–12) SW mice. Conventionalization was initiated in GF SW mice at postnatal day 21 and lasted for 7 or 21 d. The markers for sorting the splenic FO, splenic T1, and LP B cells were described in Fig. 4. Data are from four and five independent experiments for 7- and 21-d conventionalization periods, respectively. For each bar graph, the frequency of each V_H gene segment

as early as postimmunization day 7 (Fig. 9 K and L, left panels). These data suggest that the microbe-dependent change in preimmune BCR repertoire can enhance humoral responses to immunization against bacteria. This effect did not appear to be a result of an enhancement of nonspecific reactivity to immunization because OVA immunization did not lead to similar increases in OVA-reactive IgM and IgG in μMT mice receiving B cells from GF or conventionalized mice (Fig. 9 M, N).

Discussion

The preimmune BCR repertoire is the substrate upon which initial pathogen recognition takes place by B cells to elicit protective Ab responses. The molecular assembly of V region exons through V(D)J recombination generates a repertoire of vast diversity that is significantly contracted by both negative and positive BCR-mediated selection forces as B cells mature to the naive IgM$^+$ IgD$^+$ B cell stage (Cancro and Kearney, 2004). Negative selection has been shown, largely with monoclonal BCR knock-in mice, to remove autoreactive specificities through BCR receptor editing (Retter and Nemazee, 1998; Halverson et al., 2004), occurring in developing bone marrow B lineage cells. Rag2-expressing immature B cells undergoing receptor editing have also been found in the intestines of weanling mice (Wesemann et al., 2013). Although weanling gut pro-B cells occupy a similar serosal surface–proximal localization preference (Wesemann et al., 2013) as the B220$^+$ IgD$^+$ observed in the current study, the editing that occurs in this small fraction of immature B cells in the weanling gut is unlikely to account for the systemic repertoire shift at the magnitude observed here. The less well-defined positive selection process known to influence mature naive B cells after receptor editing (Cancro and Kearney, 2004) may be playing a role.

Although several studies have shown that self-antigens influence selection of MZ and B1 cells, follicular B cells are also sensitive to ligand-mediated positive selection to low affinity self-antigens (Gaudin et al., 2004a,b). The identities of B cell–selecting self-antigens are not fully known, and any selecting environmental antigens, which also have been speculated to play a role in shaping preimmune repertoires (Gu et al., 1991; Levine et al., 2000; Cancro and Kearney, 2004), have not been defined. By directly testing the degree to which symbiotic microbes influence reactivity to small intestinal bacteria in the IgM$^+$ IgD$^+$ BCR repertoire, we find that exposure to microbial symbionts endow hosts with increased antibacterial specificities in the follicular B cell pool, which can influence both mucosal and systemic immunity.

The dual approach of using LDA to measure B cell recognition of cultured small intestinal bacteria and a cellular binding assay

to assess reactivity to live bacteria-containing SIC concordantly revealed the shift toward increased reactivity to SI luminal content. A low level of conventional activation of IgM$^+$ IgD$^+$ cells giving rise to the repertoire shifts observed cannot be ruled out. However, the T cell independence, lack of memory B cell markers, absence of evidence of SHM, and lack of an increase of clonal expansion in these phenotypically naive cells are all consistent with changes within the preimmune repertoire. Also, the *BAC-Rag2pGFP* mice reveal that essentially all B cells present in mice at weaning age, regardless of tissue source, are GFP$^+$, indicating they are within 2–4 d of completing Rag-dependent *Ig* assembly (Nagaoka et al., 2000). In addition, the symbiont-induced *Ig* repertoire changes observed in the naive follicular compartment revealed by deep sequencing are largely already present at the transitional B cell stage, consistent with findings that the transition between early developing B lineage cells and mature B cells is susceptible to preimmune BCR selection (Cyster et al., 1996; Wang and Clarke, 2003; Gaudin et al., 2004a; Meyer-Bahlburg et al., 2008).

Our deep Ig sequencing data are consistent with the concept that self-antigens likely play a significant role in selecting repertoires as both GF and colonized mice had similar levels of expanded clonotypes and uneven V$_H$ gene segment preferences. Similar to a previous study (Lindner et al., 2015), we found that the IgH repertoires between individual mice are highly variable, obscuring identification of individual clones that can recognize common antigens from different mice. This is a result of the highly random nature of the part of the V exon that makes up the V(D)J junction, encoding the Ig CDR3 region. However, we found that by plotting the absolute difference in normalized V$_H$ gene segment usage frequencies between GF and colonized littermates, V$_H$ segments were identified that were likely to be influenced by microbial symbiont exposure, based on strong correlations between the day 7 and day 21 time points. These analyses suggest that much of V$_H$ preference changes that take place occur by 7 d of conventionalization (corresponding to postnatal day 28).

Our results suggest that signals and/or microbial antigens gain access to the host to influence preimmune B cell selection. During conventionalization, the intestinal mucus barrier is under dynamic development with variable permissiveness of the mucosal barrier to environmental antigens influenced by age and the microbiota. Luminal antigen availability may be enhanced in GF mice, which have been shown to have a weaker mucosal barrier (Johansson et al., 2015); however, microbial products have been shown to gain systemic access under SPF conditions (Zeng et al., 2016), which indicates that luminal antigens may directly

usage was calculated by dividing the total counts of the sequences aligned with the V$_H$ gene segment by the total counts of the sequences in the indicated conditions. The V$_H$ gene segments are not depicted if the overall usage frequencies in all the B cell subsets (T1, SpL FO, and LP) added together was less than 0.001. The V$_H$ segments (n = 90) on the x axis are aligned based on their location on chromosome arrangement from distal (left) to the most proximal (right). The individual sequencing libraries (generated from one mouse in the indicated condition) counted in the frequency were assigned with different colors in the bar graphs. The same color shown in the solid bar and the open bar in the same bar graph indicated the libraries were generated from littermates. The length of each color segment shown in the bars indicates the proportion of individual sequencing libraries contributing to the total frequency. The two blue-colored segments shown in B are generated from two technical sequencing repeats from the same library. For each bar graph, the clonal expansion (CE)–included sequences and the CE-excluded sequences were plotted on the top and the bottom, respectively. Jensen-Shannon divergences (JSDs) were calculated and p-values were assigned against permutation tests of libraries under comparison.
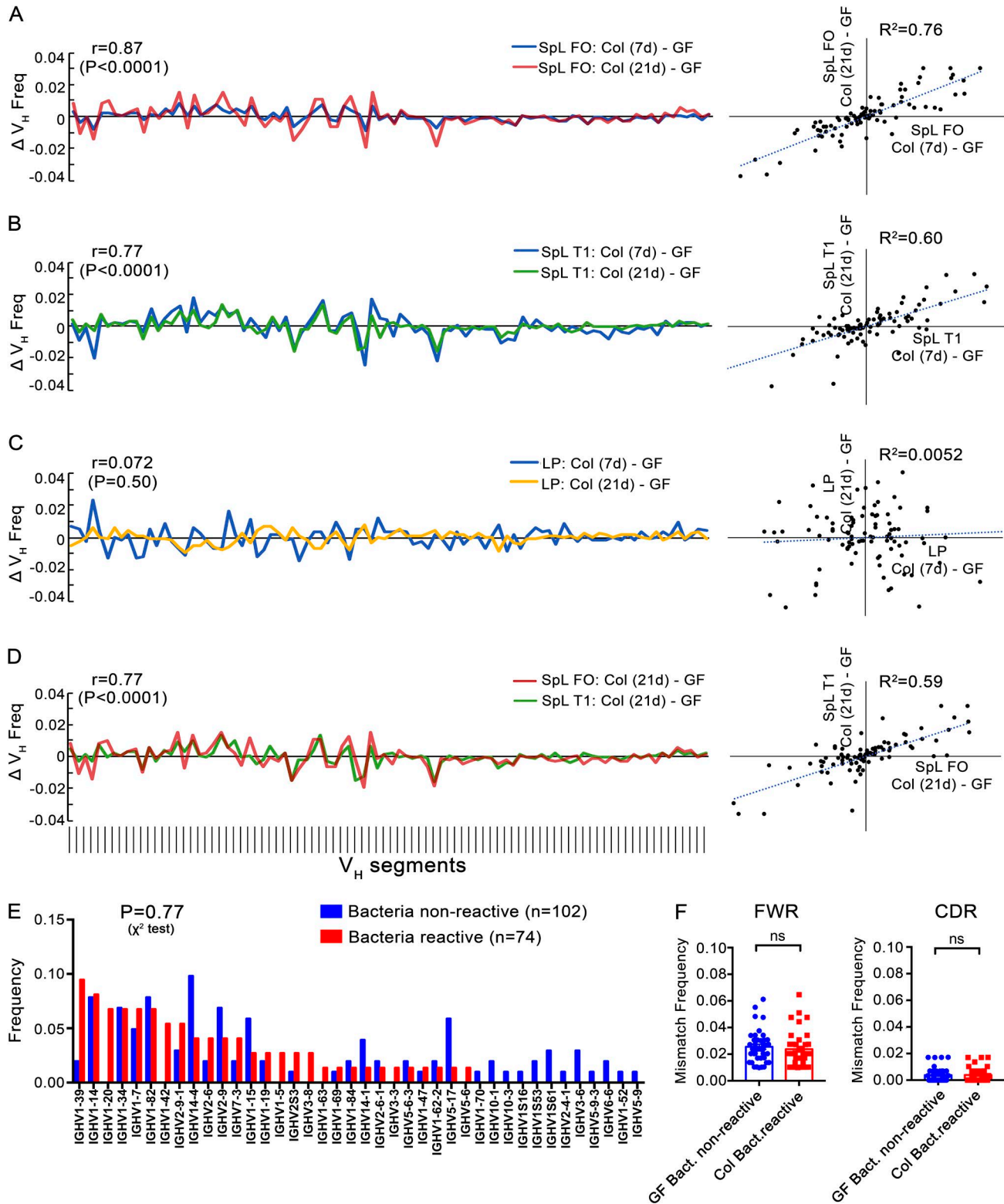
Figure 6. **Microbial symbionts influence V$_H$ usage frequencies. (A–C)** Overlay of line graphs indicating differences in V$_H$ segment usage frequencies between colonized (Col) and GF littermates (Col–GF) in the SpL follicular (FO) B cells (A), SpL transitional 1 (T1) B cells (B), and small intestinal lamina propria (LP) B cells (C) sorted from GF (n = 5–12) mice and that of conventionalized littermates (Col; n = 5–12). Conventionalization of GF mice was initiated at postnatal age day 21 for 7 or 21 d. **(D)** Overlay of the line graphs showing Col–GF subtraction plots of V$_H$ frequencies in sorted SpL FO B cells and SpL T1 cells. The markers for sorting the splenic FO, splenic T1, and LP B cells were described in Fig. 4. The correlation coefficient (R) between the two lines in each graph and its p-value are shown. The frequencies of V$_H$ segment usage were calculated as described in Fig. 5. The order of V$_H$ genes (n = 90) shown on the x axis is the same as that shown in Fig. 5. Data are from four and five independent experiments for 7- and 21-d conventionalization experiments, respectively. Only unique CDR3s were included in the subtraction plot analysis. **(E)** Bar plot showing the frequency of V$_H$ gene segments amplified from single cultured splenic B cells sorted from GF and conventionalized SW littermates. The cells for V$_H$ gene segment amplification were selected based on the reactivity of their secreted IgM toward cultured

Chen et al.
Microbial symbionts regulate the primary Ig repertoire

Journal of Experimental Medicine
https://doi.org/10.1084/jem.20171761

1406

influence the preimmune repertoire selection, but the locations and context of this potential interaction remain to be determined.

The germline-encoded array of V_H gene segments may represent anticipatory immunological sensory value selected over evolutionary time (Granato et al., 2015), with V(D)J-mediated CDR3 junctional diversity and V_H/V_L combinatorial diversity representing layers of enhanced flexibility that could cope with timescales that may be more relevant to shifting conditions of host living environments and patterns of microbial exposures. In this regard, the bacteria-reactive sequences appeared to include many V_H gene segments that were also found in nonreactive sequences, suggesting that the more flexible features of preimmune Ig diversity likely underlie much of the reactivity to small intestinal bacteria.

Somatic evolution of the preimmune Ig repertoire via secondary V exon diversification through SHM represents an additional layer of flexibility to target antigens identified in the context of focused, coordinated immune responses with timescales relevant to microbial evolution. SHM-mediated diversification could potentially compensate for holes in the primary repertoire (Silver et al., 2018), but likely through processes associated with costly delays in protective humoral responses. In this regard, purely random components of the preimmune Ig repertoire may be prone to failure without some intrinsic algorithm for anticipating protective utility (Cancro and Kearney, 2004). We propose that microbial symbiont-dependent enrichment of antimicrobial Ig specificities may represent a developmental assessment of the prospective protective utility of the randomly generated components of the primary Ig repertoire on a flexible time scale. Consistent with this notion, naive B cells from symbiont-experienced mice provided enhanced support for T cell–independent IgA to recognize small intestinal bacterial content. B cells from symbiont-exposed mice also provided an enhanced IgG response to systemic bacterial challenge, suggesting that the symbiont-induced Ig repertoire changes may be physiologically relevant. A nonmutually exclusive alternative is that microbial exposures may help regulate preimmune Ig polyreactivity, recently shown to be further enriched in the context of microbe-independent IgA development (Bunker et al., 2017).

Symbiont-influenced B cells may also have effects outside of direct bacterial recognition. Ig repertoires that appear to have been preselected toward symbiotic bacteria have been shown to prime immunodominance in the setting of HIV vaccine responses (Williams et al., 2015). In this regard, the failure of an HIV-1 vaccine trial was observed to be a result of the presence B cells reactive to a nonneutralizing epitope on the HIV-1 envelope glycoprotein gp41, which was in high relative frequency because of cross-reactivity to, and prior enrichment from, intestinal microbiota (Williams et al., 2015). How different microbial ecologies affect host–microbe homeostasis and systemic immune fitness by way of influencing Ig repertoires may be required for a more complete understanding of systemic immunity and vaccine development.
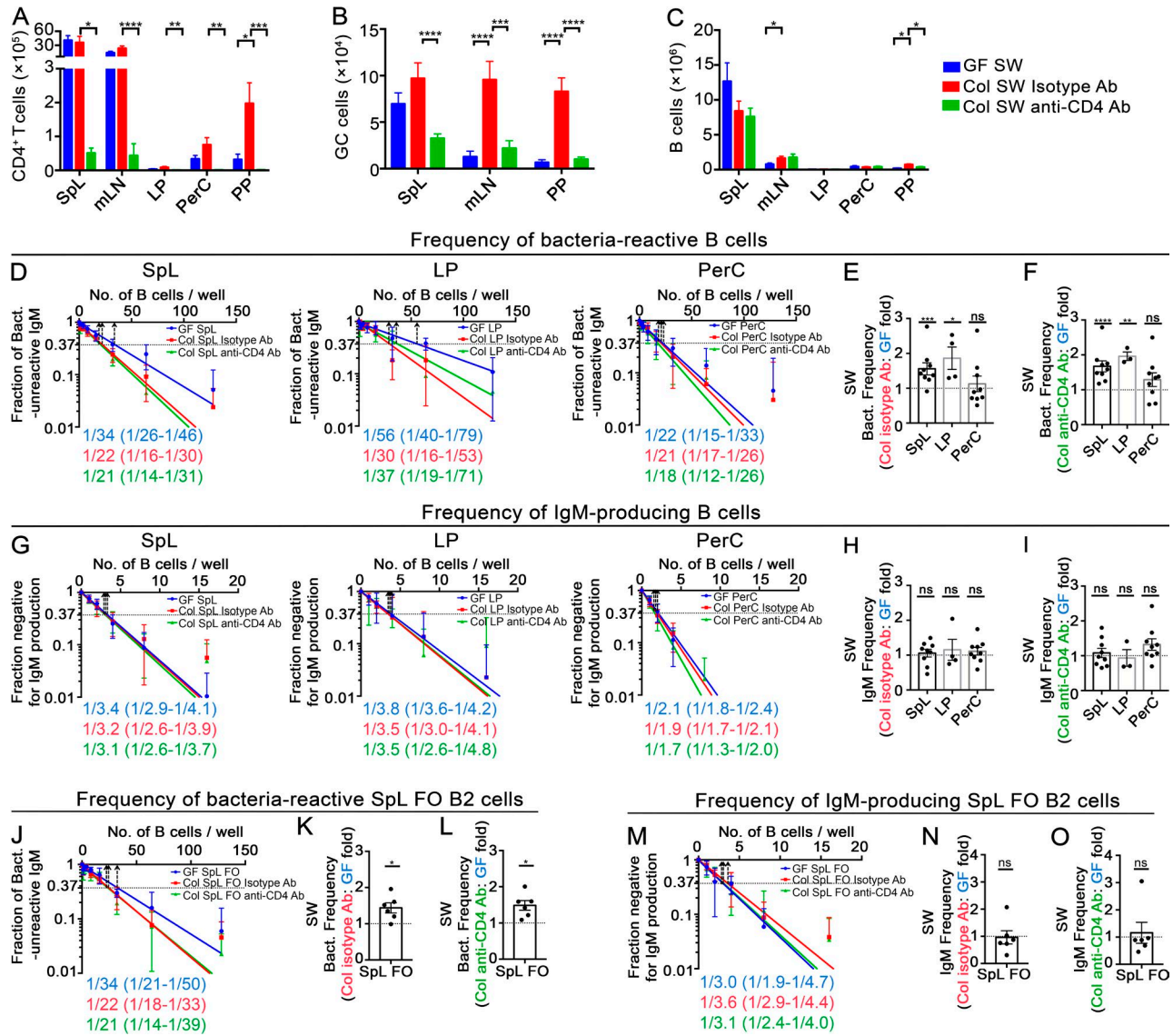
Materials and methods

Mice and conventionalization
SW mice were housed at the Boston Children's Hospital gnotobiotic facility. C57BL/6J GF mice were housed at the National Gnotobiotic Rodent Resource Center and the Boston Children's Hospital gnotobiotic facility. Littermate GF mice were randomly assigned for each GF/conventionalization experiment. Conventionalization of GF SW mice occurred by cohousing with female SPF mice in Boston Children's Hospital SPF mice facility. Conventionalized GF C57BL/6J mice were cohoused with female SPF mice at the National Gnotobiotic Rodent Resource Center or the Boston Children's Hospital SPF mice facility. For each conventionalization experiment, half of the littermates were kept in GF condition while the other half of the littermates were cohoused with the SPF mice. The GF and conventionalized littermates were analyzed at the same date after the conventionalization period was completed. The status of GF and colonization was confirmed by microbial culture, gram staining of cecal SIC, and 16S sequencing. 129S1/SvImJ mice were housed in the Boston Children's Hospital SPF mice facility. BALB/c mice were purchased from Taconic Biosciences. *BAC-Rag2pGFP* mice were described previously (Yu et al., 1999) and were purchased from Jackson Laboratories. *Rag2*$^{-/-}$ mice, described previously (Shinkai et al., 1992), were provided by F. Alt (Boston Children's Hospital, Boston, MA). B cell-deficient μMT mice (C57BL/6J) were purchased from Jackson Laboratories. Anti-hemagglutinin monoclonal mice, described previously (Curotto de Lafaille et al., 2001), were provided by J. Lafaille (New York University, New York, NY). All experiments with mice followed the protocols approved by the Boston Animal Care Facility of the Boston Children's Hospital.

Cell isolation, culture, and flow cytometry
LP and PP lymphocytes were isolated essentially as described (Wesemann et al., 2013). In brief, the small intestine was cut into pieces after excising PPs and fat. PP-excised tissue was incubated with HBSS with 1 mM EDTA and 10% FBS at room temperature three times for 8 min each to remove the intraepithelial lymphocytes. The remaining tissue was digested in RPMI containing 15% FBS (Sigma) with 0.05% collagenase D (Roche) for 45 min at 37°C twice with stirring. LP lymphocytes were enriched by centrifugation over lympholyte (Cedar Lane) to remove debris and epithelia cells. LP cells may include isolated lymphoid follicles by this extraction method. Spleen, mesenteric lymph node (mLN), and PPs were

intestinal bacteria. 74 IgH sequences were amplified from bacteria-reactive single cultured cells sorted from GF (*n* = 7 and 37 sequences) and colonized SW littermates (*n* = 7 and 37 sequences). 102 IgH sequences were amplified from bacteria nonreactive single cultured cells sorted from GF (*n* = 7 mice and 40 sequences) and colonized SW littermates (*n* = 7 mice and 62 sequences). P-value calculated from the χ² test. **(F)** Dot plot showing mismatch frequencies (compared with the germline reference sequences in IMGT) in the frame work regions 1, 2, and 3 (FWR) and the complementarity-determining regions 1 and 2 (CDR) in the sequences isolated from bacteria nonreactive single cultured splenic B cells of GF (*n* = 40) and bacteria-reactive single cultured splenic B cells of colonized (Col; *n* = 37) littermates which were cohoused with the SPF mice for 21 d beginning at the age of postnatal day 21. Two-tailed *t* test indicated no significant change. ns, not significant. Data are from five independent experiments.

Chen et al.
Microbial symbionts regulate the primary Ig repertoire

Journal of Experimental Medicine 1407
https://doi.org/10.1084/jem.20171761

Figure 7. **Microbial symbionts regulate bacteria reactivity in the primary Ig repertoire in a T cell–independent manner. (A–C)** Bar graphs showing the total number of live CD4+ T cells (A), GC B cells (DAPI− CD19+ B220+ GL7+ CD95+; B), and total B cells (DAPI− CD19+ B220+; C) in the indicated tissues from GF (blue; *n* = 14), isotype Ab–injected (red; *n* = 16), and anti-CD4 Ab–injected (green; *n* = 16) littermates colonized for 14 or 21 d. Data are from five independent experiments. *, P < 0.05; **, P < 0.01; ***, P < 0.0005; ****, P < 0.0001, multiple *t* test. Error bars indicate ± SEM. **(D–O)** LDA line graphs (D, G, J, and M), and fold-change bar graphs (E, F, H, I, K, L, N, and O) showing comparisons of frequencies of bacteria-reactive IgM (D–F and J–L) and total IgM-producing B cells (G–I and M–O) of the indicated sorted cell populations from GF mice (*n* = 4–8) or mice colonized with SPF microbiota treated with an isotype control Ab (*n* = 4–9) or a CD4 T cell-depleting anti-CD4 Ab (*n* = 3–9). Splenic B cells were sorted based on a DAPI− B220+ GL7− CD95− phenotype. Splenic follicular (FO) B cells were sorted based on the DAPI− B220+ CD93− GL7− CD95− CD43− CD23+ CD21int phenotype. Dots indicate individual mice. Data are from two to three independent experiments. P-values were calculated using the one-sample *t* test. The dashed line in the bar graphs indicates the null hypothesis. All colonization experiments were initiated at postnatal day 21 for 21 d. Numbers in graphs indicate mean frequencies (D, G, J, and M). Numbers in parenthesis (D, G, J, and M) indicate 95% confidence intervals (CI). Dotted arrows indicate the minimum number of cells required to achieve bacteria-reactive IgM (D and J) or IgM production (G and M). Error bars indicate ± 95% CI (D, G, J, and M) or ± SEM (E, F, H, I, K, L, N, and O). *, P < 0.05; **, P < 0.01; ***, P < 0.0005; ****, P < 0.0001. ns, not significant.

mashed through cell strainer (70 µm) with PBS containing 2% FBS. Peritoneal cavity cells were isolated through collecting fluids in the PerC after injecting 3 ml of PBS with 2% FBS. Splenic, mLN, PerC, and PP cells were treated with 1 mM EDTA and collagenase D similarly to the LP cells if they were analyzed in SIC binding assays to control for possible effects of the more extensive isolation procedure for LP on antigen binding. Cells were also treated stained with fluorophore or biotin-conjugated anti–mouse Ab from Biolegend, Thermo Fisher, BD Bioscience,

and MyBioSource as follows: CD19 (6D5), B220 (RA3-6B2), CD4 (GK1.5, RM4-4), CD8a (53-6.7), CD11b (M1/70), CD5 (53-7.3), CD21/CD35 (8D9), CD23 (B3B4), CD93 (AA4.1), CD43 (S7), GL7 (GL7; Thermo Fisher), CD95 (15A7), IgM (1B4B1), IgD (11-26c.2a), CD24 (30-F1), Ly-51 (6C3), IgA (C10-3), CD80 (16-10A1), PD-L2 (TY25), CD73 (TY/11.8), F(ab')2 Anti–Mouse kappa (MBS674438), and Streptavidin (Biolegend). CD19, B220, CD93, CD23, CD43, CD11b, IgM, IgD, CD80, PD-L2, and CD73 staining were tested on the bone marrow and splenic cells treated with 1 mM EDTA and collagenase
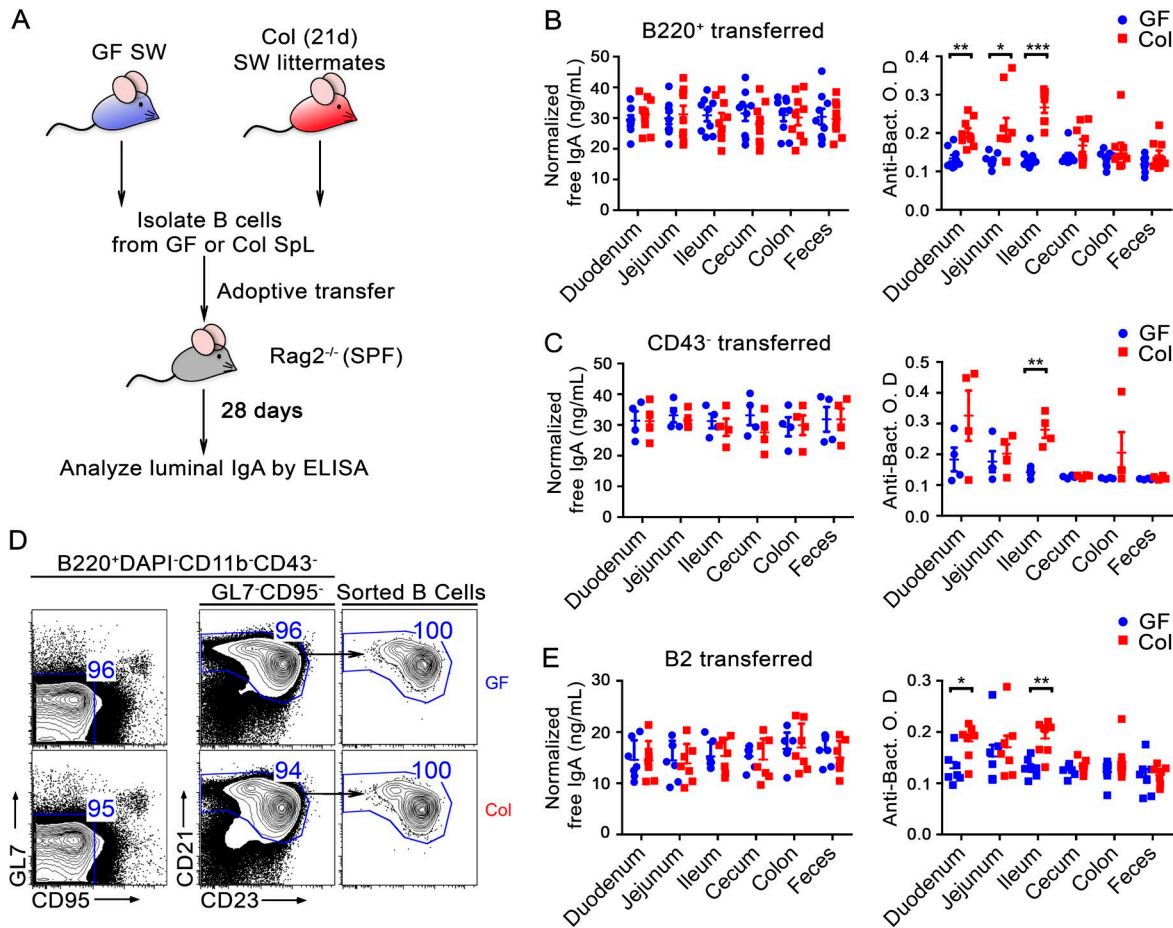
Figure 8. **Symbiotic microbes can prime naive B cells toward enriched bacteria-reactive IgA. (A)** Schematic of the adoptive transfer procedure. **(B, C, and E)** Total normalized IgA isolated from lumens of indicated intestinal sections from recipient SPF *Rag2*^{−/−} mice (left) and its reactivity to bacteria cultured from intestine (right) measured by ELISA 28 d after splenic B220^{+} (B), CD43^{−} (C), or sorted B2 cells (E) were transferred from GF SW mice (*n* = 4–9) or littermates conventionalized with SPF microbiota from the age of postnatal day 21 for 21 d (Col; *n* = 4–9). *, P < 0.05; **, P < 0.01; ***, P < 0.0005, two-tailed *t* test. Data are from two to three independent experiments. **(D)** FACS plots of the sorting strategy and the purity of sorted B2 (DAPI^{−} B220^{+} CD43^{−} CD11b^{−} GL7^{−} CD95^{−} CD21^{+}) cells.

D to confirm that the isolation procedure of LP did not influence the staining. Flow cytometry was performed on flow cytometer (Canto II; BD Bioscience). The sorting was performed on a flow cytometer (Aria II; BD Bioscience). All the isolation procedures for LP were separated from other tissues, and the staining was on separated 96-well plates. The purity of the sorted cells was above 90%. Cells were cultured in R15 medium containing RPMI, 15% FCS, 10 mM Hepes, 100 µM α-mercaptoethanol (Sigma), Streptomycin, Penicillin, glutamine, and nonessential amino acids (Gibco).

BCR internalization and SIC-binding assay
To prepare cells for SIC binding assays, 2×10^6 cells were incubated in complete RPMI containing 15% FBS and 1 µg/ml F(ab')$_2$ Anti–Mouse kappa (MyBioSource) or the isotype IgG control (Southern Biotech) at 37°C for 4 h before washing cells three times with PBS with 2% FBS at 4°C. BCR internalization was assessed by flow cytometric surface IgM mean fluorescence intensity (MFI). SIC was removed by moving forceps along the small intestine segment and collected in the Eppendorf tubes on ice. A 100-mg amount of SIC was resuspended in 1 ml PBS

by vortexing for 1 min. The suspension was centrifuged at 750 g for 5 min to remove the large debris from SIC. The supernatant from this first low-speed centrifugation was centrifuged again at 15,000 g for 1 min to enrich the bacteria-containing fraction. The high-speed centrifugation pellet was washed twice with 1 ml of 100 mM sodium bicarbonate buffer, and then resuspended in 100 µl of 100 mM sodium bicarbonate buffer. The SIC was labeled by Alexa Fluor succinimidyl esters (NHS esters; Life Technologies) following the manufacture's protocol. In brief, 100 µg NHS esters was resuspended in 15 µl DMSO to obtain a solution of ∼10 mM. Immediately, 5 µl NHS esters was added to the 100 µl bacteria-containing SIC fraction for a final concentration of 0.5 mM. The mixture of NHS esters and bacteria-containing SIC fraction was incubated at room temperature for 4 h protected from light. After the incubation, the labeled SIC was washed twice with 1 ml HBSS buffer and centrifuged at 15,000 g for 1 min. The pellet was resuspended with 100 µl PBS and the aliquots were stored at −80°C. 0.5×10^6 of F(ab')2 anti–mouse Igκ–treated, or isotype control Ab–treated cells, were incubated with 0.5 µl labeled SIC on ice for 20 min in 50 µl PBS with 2% FBS. The cells were washed three times with PBS 2% FBS at 4°C. The cells were

Chen et al.
Microbial symbionts regulate the primary Ig repertoire

Journal of Experimental Medicine
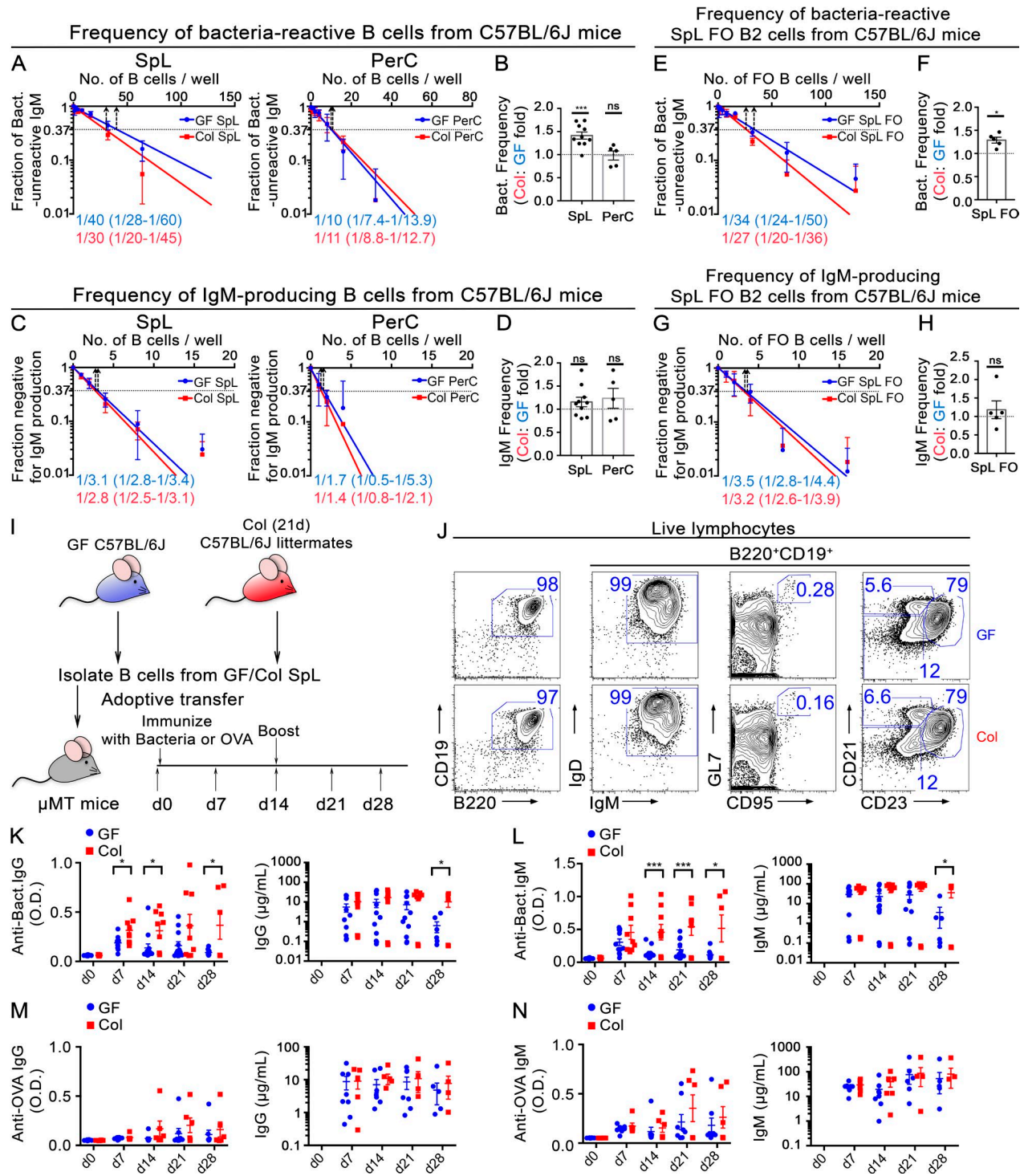https://doi.org/10.1084/jem.20171761

1409

Figure 9. **Symbiotic microbes prime naive B cells toward higher systemic immune response against bacteria. (A–D)** LDA line graphs (A and C) and fold-change bar graphs (B and D) of DAPI⁻ B220⁺ cells sorted from the SpL (n = 10) and PerC (n = 5) of GF and colonized (Col) C57BL/6J littermates for IgM reactivity to intestinal bacteria (A and B) or total IgM (C and D). Data are from two to three independent experiments. **(E–H)** LDA line graphs (E and F) and fold-change bar graphs (G and H) of splenic follicular (FO) B cells (DAPI⁻ B220⁺ CD93⁻ CD95⁻ GL7⁻ CD43⁻ CD23⁺ CD21^{int}) sorted from SpLs of GF (n = 5) and colonized C57BL/6 littermates (Col; n = 5) for IgM reactivity to intestinal bacteria (E and F) or total IgM (G and H). Data are from two independent experiments. P-values calculated using the one-sample t test. **(I)** Schematic of the adoptive transfer and immunization procedure. **(J)** FACS plots of the purity and composition of the purified B cells for adoptive transfer. The plots shown are representative of three independent adoptive transfer experiments. **(K–N)** ELISA data showing antibacterial IgG (K) and IgM (L) or total IgG (K) and IgM (L) from intestinal bacteria-immunized SPF μMT that received splenic B220⁺ B cells from GF C57BL/6J (n = 8–12) or colonized littermates (Col; n = 6–9). Control experiments using OVA immunization and anti-OVA Ab were also performed in parallel (M and N). Each dot represents an individual mouse from two to three independent adoptive transfer experiments for bacteria or OVA immunization experiments, respectively. P-values calculated using the two-tailed t test. The dashed line in the bar graphs indicates the null hypothesis. In the LDA experiments, numbers in graphs (A, C, E, and G) indicate mean frequencies. Numbers in parenthesis (A, C, E, and G) indicate the 95% confidence

Chen et al.
Microbial symbionts regulate the primary Ig repertoire

Journal of Experimental Medicine

1410

https://doi.org/10.1084/jem.20171761

stained with surface markers as indicated and DAPI afterward and then processed flow cytometrically.

Bacteria culture

Intestinal content from SW mice colonized mice was weighed and resuspended in 1 ml sterile PBS. Large debris was removed by centrifuging the resuspension at 750 g for 5 min. The supernatant from this first low-speed spin was collected and centrifuged with higher speed at 10,000 g for 1 min to pellet bacteria. The pellet was resuspended in 1 ml PBS per 1 g of original intestinal content and inoculated by glass pipet into glass tubes containing 12 ml of semisolid thioglycolate medium (Sigma). Tubes were sealed in ambient conditions before incubation at 37°C for 5–7 d. The bacteria were harvested by centrifugation at 10,000 g for 5 min. The liquid and agar layers were removed by aspiration and the bacterial pellet was resuspended sterile PBS with 20% glycerol for storage at –80°C.

Immunofluorescence microscopy

Small intestines were washed twice in PBS after gently removing the fat and SIC. The small intestines were fixed in 4% paraformaldehyde (PFA) for 2 h at room temperature, incubated in 30% sucrose overnight at 4°C, and then frozen in optimal cutting temperature compound (Thermo Fisher). The intestinal sections were cut at 16 µm using cryostat (CM3050; Leica Microsystems) and mounted on the superfrost plus slides (Thermo Fisher). Sections were washed in PBS and permeabilized with 0.2% Triton X-100 (Thermo Fisher) for 5 min. After washing the slides three times with wash buffer (2% BSA plus 0.02% Tween), the sections were blocked with 2% BSA for 1 h and then stained with the specific fluorophore-conjugated Ab in 2% BSA for 1 h. The Ab were FITC-IgA (11-44-2; Southern Biotech), PE-IgD (11-20-09; Southern Biotech), and APC-B220 (17-0452-83; Thermo Fisher). After the staining, the slides were washed three times with wash buffer and then mounted in fluoromount G with DAPI (Thermo Fisher). Images were acquired with LSM 800 with Airyscan confocal system on an Axio Observer Z1 inverted microscope (Zeiss). Quantification of IgA+ and IgD+ cells were performed blindly using the Zen Lite software and ImageJ (National Institutes of Health). Individual cells (IgA+, IgD+, B220+, and IgD+B220+) were counted using Zen Lite software (Zeiss). Cells were counted as part of the LP cells if they were positioned above the inner side of serosal surface. The IgD+ cells in PPs or isolated lymphoid follicles were not considered as LP B cells. The IgA+ or IgD+ B200+ cells per high power field per mouse was calculated by dividing total number of IgA+ or IgD+ B200+ cells per mouse over the number of high-power fields counted. The analysis of distance of cells to the serosal surface was done on ImageJ. The scale bars were consistent, using both Zen Lite and ImageJ. The inner side of serosal surface was first identified and labeled with a straight line. A perpendicular line was drawn, connecting each cell to the serosal line. The length of this perpendicular line, corresponding to the distance

of the cell to the serosa surface, was measured in micrometers. If the serosal surface underneath the cell was not captured in the image, a parallel line to the serosal line was drawn and extended over the area where the serosal surface was visualized. A similar perpendicular line, resembling the distance of cell to the serosa, was measured in micrometers.

Microbial community analysis

Total DNA was isolated from 100 mg SIC, 100 mg cecal content (CC), bacteria cultured from SIC (SIB), bacteria cultured from CC (CCB), and the 1:1 ratio mixture of SIB and CCB (BAC) of the conventionalized SW, beginning at the age of 21–22d for 21 d or the SPF 129S1/SvImJ mice cohousing with the GF SW mice for the conventionalization. SIB and CCB were resuspended in 500 µl sterile PBS to reach OD_{600} = 0.5, from which 100 µl were collected for the DNA isolation. SIB and CCB were then mixed at 1:1 ratio (BAC) from which 100 µl were collected for total DNA isolation. SIC and CC were resuspended in 1 ml sterile PBS. Large debris was removed by centrifugation at 750 g for 5 min. Supernatants were then centrifuged at 10,000 g for 1 min to collect microbes. The pellets from SIC and CC, as well as the cultured bacteria, were resuspended in TE buffer containing Lysozyme (5 mg/ml) and incubated at 37°C for 45 min, followed by 1 h at 56°C with 0.5 mg/ml proteinase K before adding 1% (wt/vol) SDS and incubating for an additional 30 min at 37°C. The DNA was extracted from the mixture and precipitated overnight with 3 M sodium acetate and washed with 70% ethanol. V4 region of 16S rRNA genes from extracted DNA were sequenced by Illumina MiSeq. The Illumina reads were demultiplexed based on sample barcodes. Paired end reads were merged using PEAR (v. 0.9.10). Unpaired reads, sequences with terminal base quality of <20, and sequences <350 bps were excluded from analysis. The filtered sequences were clustered into operational taxonomic units at 97% similarity using the Greengene database using Quantitative Insights into Microbial Ecology version 1.9.1.

Single cell culture and LDA

For both single cell culture and LDA, 3×10^3 irradiated S17 cells (provided by A. Nobrega, Federal University of Rio de Janeiro, Rio de Janeiro, Brazil, and H. Schroeder, University of Alabama at Birmingham, Birmingham, AL) were plated on each well of 96-well (flat) plates in R15 with 10 µg/ml LPS (Sigma) 4–6 h before plating B cells. For the single cell culture, single cells from the desired B cell populations were sorted on the feeder cells. For the LDA, 22~48 replicates of 1, 2, 4, 8, 16, 32, 64, and 128 B cells with either magnetically purified B220+ cells or flow cytometrically sorted B cells defined with the markers as indicated in the text were plated or sorted onto S17 feeder cells. SpL, LP, or PerC cells from 1~4 GF or 1~4 conventionalized mice were pooled for each experiment. The cells were incubated at 37°C with 5% CO_2 for 5–7 d. Supernatants were collected after the incubation and tested by ELISA. The cell dose yielding 37% negative binding to

interval (CI). Dotted arrows indicate the minimum number of cells required to produce bacteria-reactive IgM (A and E) or IgM production (C and G). Error bars indicate ± 95% CI (A, C, E, and G) or ± SEM (B, D, F, H, and K–N). *, P < 0.05; ***, P < 0.001. Conventionalized GF C57BL/6J mice were cohoused with the SPF mice for 21 d beginning at the age of postnatal day 21 to 25.

anti-IgM gave a frequency of IgM-producing cells. The IgM-producing cell dose yielding 37% negative binding to bacteria gave the frequency in the population capable of responding to bacteria as described (Vale et al., 2012).

RT-PCR amplification of V_H genes from single cell culture

Single splenic B cells (DAPI⁻B220⁺) were sorted on the 96-well (flat) plates with 3×10^3 irradiated S17 feeder cells incubated with R15 medium containing 10 µg/ml LPS (Sigma) as described above. After 5 d of incubation at 37°C with 5% CO_2, the plates were centrifuged at 1,000 rpm for 5 min at 4°C. After transferring the supernatants, the pellets were lysed with 10 µl/well of ice-cold 0.5 × PBS containing 10mM dithiothreitol and 4 U RNAaseout (Thermo Fisher). The lysed pellets were immediately frozen on dry ice and stored at –80°C. Based on the ELISA results, 4 µl of the lysates from all the original wells producing bacteria-reactive IgM and a proportion of the wells producing bacteria-nonreactive IgM were processed for reverse transcription. The first-strand cDNA was synthesized in a final volume of 10 µl/well using 10 µM primer specific for the µ constant region (3′ Cµ outer, 5′-AGGGGG CTCTCGCAGGAGACGAGG-3′; Tiller et al., 2009),1 mM dNTP (Promega), 10 mM dithiothreitol (Thermo Fisher), 0.5% vol/vol Igepal CA-630 (Sigma), 12 U RNAaseout (Thermo Fisher), and 40 U Superscript III reverse transcription (Thermo Fisher). The reverse transcription reactions were performed at 50°C for 2 h, 70°C for 15 min, and stored at –80°C. *Igh* gene transcripts were amplified by two rounds of seminested PCR starting from 2 µl of cDNA as the template in 20 µl of reaction. Followed by Hotstart Taq (Qiagen) activation at 95°C for 15 min, the first round of PCR was performed for 50 cycles of 94°C for 30s, 56°C for 30s, 72°C for 55s, and final extension at 72°C for 10 min. Primers for amplification were 5′ MsVHE (5′-GGGAATTCGAGGTGCAGCTGC AGGAGTCTGG-3′) and 3′ Cµ outer. 2 µl of unpurified first round PCR product was used for the seminested second round PCR, starting with Hotstart Taq (Qiagen) activation at 95°C for 15 min. The reactions were then performed for 50 cycles of 94°C for 30 s, 45°C for 30 s, 72°C for 45 s, and final extension at 72°C for 10 min. Primers for amplification were 5′ MsVHE and 3′ Cµ inner (5′-AGGGGGAAGACATTTGGGAAGGAC-3′; Tiller et al., 2009). Final PCR products were analyzed by 1% agarose gels. Aliquots of the PCR product were purified using QIAquick PCR purification kit (Qiagen) and sequenced with the reverse primer 3′ Cµ inner. The nucleotide sequences were analyzed by using ImMunoGeneTics (IMGT)/V-Quest to identify the highest homologous germline IgH V, D, and J gene segment.

High throughput BCR repertoire sequencing

B cell subsets from GF and conventional littermates were sorted on flow cytometer (Aria II; BD Bioscience) as follows: splenic T1 B cells (DAPI⁻CD19⁺IgM⁺B220^low CD93⁺CD23⁻), splenic FO B cells (DAPI⁻CD19⁺IgM⁺B220⁺CD95⁻CD43⁻CD93⁻CD23⁺CD21^int), and LP FO B cells (DAPI⁻CD19⁺IgM⁺B220⁺CD95⁻GL7⁻CD93⁻CD23⁺). Total RNA was extracted from sorted B cells using TRIzol reagents (Thermo Fisher). A total of 0.1 to 1 µg RNA/sample was used for the first-strand cDNA synthesis by using oligo dT and Superscript III reverse transcription (Thermo Fisher) following the manufacture's instruction. The first-strand cDNA

was purified by the Agencourt RNAClean XP (Beckman) beads to remove the primers. 19 forward degenerate primers binding to the framework region 1 of the VH region (Krebber et al., 1997; Greiff et al., 2014) barcoded by an eight-nucleotide UMI and connected with the universal primer (FW-UNV, 5′-AAGCAGTGG TATCAACGCAGAG-3′) were used for the second strand cDNA synthesis. Following Hotstart Taq (Qiagen) activation for 15 min at 95°C, primer annealing for 90 s at 60°C, and extension for 10 min at 72°C, the reaction was then purified again by the Agencourt RNAClean XP beads (Beckman) to remove the barcoded primers. The first round of PCR was performed using Phusion DNA polymerase (Thermo Fisher) and one fourth of the barcoded cDNA with 25 cycles of 98°C for 10s, 62°C for 30s, and 72°C for 30s. The primers were forwarded primer Fw-CS1-UNV (5′-TACACTGACGACATGGTTCTACAAAGCAGT GGTATCAACG-3′) and Rv-I7-Cµ primer (5′TACGGTAGCAGAGAC TTGGTCTAGTAGGGGGAAGACATTTGGGAAGGAC-3′), which anneals to µ constant region. For the samples exacted from LP, preamplification was performed before the first-round PCR using Phusion DNA polymerase and the barcoded cDNA by the primer Fw-UNV and 3′Cµ outer (Tiller et al., 2009) with nine cycles of 98°C for 10s, 55°C for 30s, and 72°C for 30s. The first-round PCR product was purified using the QIAquick PCR purification kit (Qiagen). The purified first-round PCR products were then subjected to the second nested PCR with Phusion DNA polymerase to add adaptors P5 (primer P5-CS1: 5′-AATGATACG GCGACCACCGAGATCTACACTGACGACATGGTTCTACA-3′) at the 5′ end and P7 (primer P7-I7: 5′-CAAGCAGAAGACGGCATACGA GATTAAGGCGATACGGTAGCAGAGACTTGGTCT-3′) at the 3′ end with sample barcode for 18 cycles of 98°C for 10s, 62°C for 30s, and 72°C for 30s. PCR products (sized between 380–700 bp) were extracted from agarose gel, and the concentration was measured by bioanalyzer. Amplicon from each library were combined and used for MiSeq v3 250 and 300 nt paired-end reads sequencing per the manufacture instruction.

Repertoire analysis

The sequences obtained from Illumina MiSeq deep sequencing were merged using PEAR v 0.9.10. The paired-end reads were truncated at the ends if the residues had a Phred score of less than 20. The merge criteria included minimum overlap of 20 nucleotides and a minimum merged length of 80 nt. The intermittent low score (<20) nucleotides were replaced by "N". All sequences with four consecutive Ns were truncated at that point. All sequences, which had more Ns than 2% of their length, were discarded. All filtered sequences were run through the standalone IgBlast software (version 1.4.0) to identify the V_H segment using reference sequences from IMGT. Igblast results with scores >40 were considered for further analysis. PCR repeats were excluded using the UMIs. Any sequences with the same V and J segment, same CDR3 region (a mismatch of two nts was allowed to account for PCR error), and same UMI sequence were considered PCR repeats, and only one copy was included for analysis. The CDR3 definition used here is 26 nts segment upstream of the J region. Sequences were considered as clonal expansion if they had the same V, same J, and same CDR3 sequence (a mismatch of one nt was allowed to account for PCR error) but different UMI.

Chen et al.
Microbial symbionts regulate the primary Ig repertoire

Journal of Experimental Medicine
https://doi.org/10.1084/jem.20171761

1412

Sequences were considered as unique clonotypes if they had unique CDR3s (clonal expansion excluded). All the analysis was done on Bioconductor package v 3.4 (R version 3.3.1).

CD4 T cell depletion

Day 21–22 GF SW mice were individually i.p. injected with 150 µg anti–mouse CD4 functional purified grade Ab (GK1.5, eBiosciences) or Rat IgG2bκ functional purified grade isotype control (eB149/10H5; eBiosciences) before the mice were cohoused with the SPF mice for conventionalization while littermates were maintained GF. The cohoused mice were injected with 100 µg anti-CD4 Ab (GK1.5) or isotype control every 3 d for the duration of conventionalization. After 14 or 21 d, the GF and colonized littermates were euthanized, and the cells from indicated tissues were harvested. The reduction of the number and frequency of CD4⁺ cells in the anti-CD4 Ab injected group was confirmed by FITC–anti-CD4 (RM4-4), which recognizes different epitope of CD4 compared with GK1.5. The harvested cells were analyzed by the SIC binding protocol or LDA described above.

Adoptive transfer

For adoptive transfer to $Rag2^{-/-}$ mice, splenocytes from four GF and four conventionalized littermates (21 d) were isolated as described above, pooled separately, and subsequently incubated with B220 or CD43 microbeads and purified through magnetic columns (Miltenyi Biotec) for isolation of B220⁺ positively selected or CD43⁻ negatively selected B cells, respectively. The purity of the cells was analyzed by flow cytometry. The purity of the sorted cells was >90% for all samples. Alternatively, naive B2 cells (B220⁺DAPI⁻CD43⁻CD11b⁻CD95⁻GL7⁻CD21⁺) were sorted from the GF and conventionalized splenocytes (21 d) pooled from four mice each. For transfer, 6×10^6 B220⁺ cells, CD43⁻ B cells, or 1×10^6 sorted B2 cells were transferred into SPF $Rag2^{-/-}$ mice by retroorbital injection. Blood and feces were collected every 7 d after the transfer. The transferred mice were euthanized 28 d after the transfer. The intestines of the transferred mice were cut into duodenal, jejunal, ileal, cecal, and colonic sections. Luminal contents from these sections, as well as fecal matter (50 mg for each), were resuspended in 200 µl PBS by vortex. The suspension was centrifuged at 10,000 g for 2 min to remove the large fragments. The supernatant was collected and diluted serially to determine the free IgA concentration by ELISA. The IgA concentration was equalized and aliquoted before being used to measure the bacteria reactivity by ELISA. For adoptive transfer to µMT mice and immunization, splenocytes from six GF and six conventionalized littermates (3 wk old) were isolated as described above, pooled separately and subsequently incubated with B220 microbeads, and purified through magnetic columns (Miltenyi Biotec) for isolation of B220⁺ positively selected B cells. The purity of the cells was analyzed by flow cytometry. For transfer, 1×10^7 B220⁺ cells were transferred into SPF µMT mice by retroorbital injection. The first immunization with cultured bacteria from small intestine and cecal cultures was performed immediately (day 0) by i.p. injection after the adoptive transfer. The boost was performed on day 14. For each immunization, the bacteria were suspended in 500 µL PBS to reach $OD_{600} = 0.5$, from which

100 µl were mixed with 100 µl Imject Alum (Thermo Fisher) before injection. 100 µl PBS was mixed with 100 µl Imject Alum (Thermo Fisher) as the control. Blood was collected every 7 d after the transfer and centrifuged at 400 g. The plasma was collected and stored at –80°C. The plasma collected from day 0 to day 21 was diluted from 1:100 to 1:100,000 for ELISA.

ELISA

Anti-IgM (1 µg/ml, Abcam, ab97226) and anti-IgG (1 µg/ml, BD, 405301) were coated on c96 Maxisorp Nunc Immuno ELISA plates (Thermo Fisher) in 30 µl of 100 mM sodium bicarbonate buffer per well at 4°C overnight. Given the yield limitations of the semisolid culture conditions for small intestinal bacteria (see Bacteria culture and labeling section) together with the large amount of ELISAs required, the bacteria used in the ELISAs of the single cell and LDA experiments were derived from both small intestine (SIB^Col) and cecal cultures (CCB^Col) in a 1:1 OD_{600} ratio we refer to as BAC, which largely consists of $Lactobacillus$, Enterobacteriaceae, and $Enterococcus$ (Fig. S1 L). Bacteria were resuspended in 500 µl PBS to reach $OD_{600} = 0.5$, from which 20 µl were resuspended in 3 ml PBS to coat each well of one ELISA plate with 30 µl per well. The plates were incubated at 37°C overnight as described (Elder et al., 1982) for drying before washing three times with PBS 0.05% Tween-20 and blocking with 3% BSA in PBS at room temperature for 3 h. The plates were then washed twice with PBS 0.05% Tween-20 before supernatants from cultures or intestinal content were added to the plates for overnight incubation at 4°C. Plates were then washed three times in PBS 0.05% Tween-20 before incubation with alkaline phosphate–labeled secondary Ab (Abcam) before another three rounds of washing and incubation with phosphatase substrate (Sigma). For the single cell cultures and limiting dilution assays, supernatants from S17 cells were used as negative controls. For the bacteria-reactive IgG or IgM detection after adoptive transfer and immunization in µMT mice, the plasma was diluted by 1:100 with 1% BSA to incubate with the bacteria coated ELISA plates. The cut-off OD was determined to be the mean of the negative control wells plus three standard deviations, above which OD values were considered positive.

Statistical analysis

If not otherwise stated, data were expressed as arithmetic means ± SEM, and statistical analyses were made by unpaired t test, Mann-Whitney test, and χ^2 test (Prism 6; Graphpad) where appropriate. Nonlinear regression fit LDA plots. P < 0.05 was considered statistically significant. Error bars indicate ± SEM unless otherwise indicated.

Data availability

The Illumina MiSeq raw sequence data for this study is accessible at the NCBI Sequence Read Archive under BioProject accession no. PRJNA422108. The immunoglobulin heavy chain sequences have the BioSample accession nos. from SAMN08167392 to SAMN08167475 and the 16S rRNA gene sequences are under the BioSample accession nos. SAMN08276854 to SAMN08276889. The heavy chain Sanger sequences are available in GenBank under the accession nos. MG675261 to MG675436. Source code for

Chen et al.
Microbial symbionts regulate the primary Ig repertoire

Journal of Experimental Medicine
https://doi.org/10.1084/jem.20171761

1413

sequence analysis can be found at https://github.com/Wesemann-lab/Immunoglobulin-repertoire-VH-segment-usage-analysis.

Online supplemental material
Fig. S1 Describes the flow cytometric assay to measure BCR-dependent binding of SIC to B cell surfaces and shows 16S data of bacterial populations. Fig. S2 displays BCR-dependent binding of SIC to B cell surfaces in GF versus conventionalized mice. Fig. S3 displays CD4 T cell depletion in anti-CD4 Ab-injected, colonized mice. Fig. S4 shows adoptive transfer of GF and conventionalized littermate B cells to $Rag2^{-/-}$ mice. Table S1 shows a summary of Ig repertoire sequencing of sorted B cell subsets from GF versus conventionalized SW littermates for 7 d or 21 d.

References
Anderson, S.M., M.M. Tomayko, A. Ahuja, A.M. Haberman, and M.J. Shlomchik. 2007. New markers for murine memory B cells that define mutated and unmutated subsets. *J. Exp. Med.* 204:2103–2114. https://doi.org/10.1084/jem.20062571

Arnold, L.W., C.A. Pennell, S.K. McCray, and S.H. Clarke. 1994. Development of B-1 cells: segregation of phosphatidyl choline-specific B cells to the B-1 population occurs after immunoglobulin gene expression. *J. Exp. Med.* 179:1585–1595. https://doi.org/10.1084/jem.179.5.1585

Baumgarth, N. 2010. The double life of a B-1 cell: self-reactivity selects for protective effector functions. *Nat. Rev. Immunol.* 11:34–46. https://doi.org/10.1038/nri2901

Bunker, J.J., T.M. Flynn, J.C. Koval, D.G. Shaw, M. Meisel, B.D. McDonald, I.E. Ishizuka, A.L. Dent, P.C. Wilson, B. Jabri, et al. 2015. Innate and Adaptive Humoral Responses Coat Distinct Commensal Bacteria with Immunoglobulin A. *Immunity.* 43:541–553. https://doi.org/10.1016/j.immuni.2015.08.007

Bunker, J.J., S.A. Erickson, T.M. Flynn, C. Henry, J.C. Koval, M. Meisel, B. Jabri, D.A. Antonopoulos, P.C. Wilson, and A. Bendelac. 2017. Natural polyreactive IgA antibodies coat the intestinal microbiota. *Science.* 358:eaan6619. https://doi.org/10.1126/science.aan6619

Cancro, M.P., and J.F. Kearney. 2004. B cell positive selection: road map to the primary repertoire? *J. Immunol.* 173:15–19. https://doi.org/10.4049/jimmunol.173.1.15

Curotto de Lafaille, M.A., S. Muriglan, M.J. Sunshine, Y. Lei, N. Kutchukhidze, G.C. Furtado, A.K. Wensky, D. Olivares-Villagómez, and J.J. Lafaille. 2001. Hyper immunoglobulin E response in mice with monoclonal populations of B and T lymphocytes. *J. Exp. Med.* 194:1349–1360. https://doi.org/10.1084/jem.194.9.1349

Cyster, J.G., J.I. Healy, K. Kishihara, T.W. Mak, M.L. Thomas, and C.C. Goodnow. 1996. Regulation of B-lymphocyte negative and positive selection by tyrosine phosphatase CD45. *Nature.* 381:325–328. https://doi.org/10.1038/381325a0

Dammers, P.M., A. Visser, E.R. Popa, P. Nieuwenhuis, and F.G. Kroese. 2000. Most marginal zone B cells in rat express germline encoded Ig VH genes and are ligand selected. *J. Immunol.* 165:6156–6169. https://doi.org/10.4049/jimmunol.165.11.6156

Elder, B.L., D.K. Boraker, and P.M. Fives-Taylor. 1982. Whole-bacterial cell enzyme-linked immunosorbent assay for Streptococcus sanguis fimbrial antigens. *J. Clin. Microbiol.* 16:141–144.

Gaudin, E., Y. Hao, M.M. Rosado, R. Chaby, R. Girard, and A.A. Freitas. 2004a. Positive selection of B cells expressing low densities of self-reactive BCRs. *J. Exp. Med.* 199:843–853. https://doi.org/10.1084/jem.20030955

Gaudin, E., M. Rosado, F. Agenes, A. McLean, and A.A. Freitas. 2004b. B-cell homeostasis, competition, resources, and positive selection by self-antigens. *Immunol. Rev.* 197:102–115. https://doi.org/10.1111/j.0105-2896.2004.0095.x

Granato, A., Y. Chen, and D.R. Wesemann. 2015. Primary immunoglobulin repertoire development: time and space matter. *Curr. Opin. Immunol.* 33:126–131. https://doi.org/10.1016/j.coi.2015.02.011

Greiff, V., U. Menzel, U. Haessler, S.C. Cook, S. Friedensohn, T.A. Khan, M. Pogson, I. Hellmann, and S.T. Reddy. 2014. Quantitative assessment of the robustness of next-generation sequencing of antibody variable gene repertoires from immunized mice. *BMC Immunol.* 15:40. https://doi.org/10.1186/s12865-014-0040-5

Gu, H., D. Tarlinton, W. Müller, K. Rajewsky, and I. Förster. 1991. Most peripheral B cells in mice are ligand selected. *J. Exp. Med.* 173:1357–1371. https://doi.org/10.1084/jem.173.6.1357

Halverson, R., R.M. Torres, and R. Pelanda. 2004. Receptor editing is the main mechanism of B cell tolerance toward membrane antigens. *Nat. Immunol.* 5:645–650. https://doi.org/10.1038/ni1076

Hayakawa, K., M. Asano, S.A. Shinton, M. Gui, D. Allman, C.L. Stewart, J. Silver, and R.R. Hardy. 1999. Positive selection of natural autoreactive B cells. *Science.* 285:113–116. https://doi.org/10.1126/science.285.5424.113

Hooper, L.V., D.R. Littman, and A.J. Macpherson. 2012. Interactions between the microbiota and the immune system. *Science.* 336:1268–1273. https://doi.org/10.1126/science.1223490

Johansson, M.E., H.E. Jakobsson, J. Holmén-Larsson, A. Schütte, A. Ermund, A.M. Rodríguez-Piñeiro, L. Arike, C. Wising, F. Svensson, F. Bäckhed, and G.C. Hansson. 2015. Normalization of Host Intestinal Mucus Layers Requires Long-Term Microbial Colonization. *Cell Host Microbe.* 18:582–592. https://doi.org/10.1016/j.chom.2015.10.007

Kitamura, D., J. Roes, R. Kühn, and K. Rajewsky. 1991. A B cell-deficient mouse by targeted disruption of the membrane exon of the immunoglobulin mu chain gene. *Nature.* 350:423–426. https://doi.org/10.1038/350423a0

Krebber, A., S. Bornhauser, J. Burmester, A. Honegger, J. Willuda, H.R. Bosshard, and A. Plückthun. 1997. Reliable cloning of functional antibody variable domains from hybridomas and spleen cell repertoires employing a reengineered phage display system. *J. Immunol. Methods.* 201:35–55. https://doi.org/10.1016/S0022-1759(96)00208-6

Levine, M.H., A.M. Haberman, D.B. Sant'Angelo, L.G. Hannum, M.P. Cancro, C.A. Janeway Jr., and M.J. Shlomchik. 2000. A B-cell receptor-specific selection step governs immature to mature B cell differentiation. *Proc. Natl. Acad. Sci. USA.* 97:2743–2748. https://doi.org/10.1073/pnas.050552997

Lindner, C., I. Thomsen, B. Wahl, M. Ugur, M.K. Sethi, M. Friedrichsen, A. Smoczek, S. Ott, U. Baumann, S. Suerbaum, et al. 2015. Diversification of memory B cells drives the continuous adaptation of secretory antibodies to gut microbiota. *Nat. Immunol.* 16:880–888. https://doi.org/10.1038/ni.3213

Macpherson, A.J., D. Gatto, E. Sainsbury, G.R. Harriman, H. Hengartner, and R.M. Zinkernagel. 2000. A primitive T cell-independent mechanism of intestinal mucosal IgA responses to commensal bacteria. *Science.* 288:2222–2226. https://doi.org/10.1126/science.288.5474.2222

Martin, F., and J.F. Kearney. 2000. Positive selection from newly formed to marginal zone B cells depends on the rate of clonal production, CD19, and btk. *Immunity.* 12:39–49. https://doi.org/10.1016/S1074-7613(00)80157-0

Meyer-Bahlburg, A., S.F. Andrews, K.O. Yu, S.A. Porcelli, and D.J. Rawlings. 2008. Characterization of a late transitional B cell population highly sensitive to BAFF-mediated homeostatic proliferation. *J. Exp. Med.* 205:155–168. https://doi.org/10.1084/jem.20071088

Nagaoka, H., G. Gonzalez-Aseguinolaza, M. Tsuji, and M.C. Nussenzweig. 2000. Immunization and infection change the number of recombination activating gene (RAG)-expressing B cells in the periphery by altering immature lymphocyte production. *J. Exp. Med.* 191:2113–2120. https://doi.org/10.1084/jem.191.12.2113

Pabst, O. 2012. New concepts in the generation and functions of IgA. *Nat. Rev. Immunol.* 12:821–832. https://doi.org/10.1038/nri3322

Retter, M.W., and D. Nemazee. 1998. Receptor editing occurs frequently during normal B cell development. *J. Exp. Med.* 188:1231–1238. https://doi.org/10.1084/jem.188.7.1231

Shinkai, Y., G. Rathbun, K.P. Lam, E.M. Oltz, V. Stewart, M. Mendelsohn, J. Charron, M. Datta, F. Young, A.M. Stall, et al. 1992. RAG-2-deficient mice lack mature lymphocytes owing to inability to initiate V(D)J rearrangement. *Cell.* 68:855–867. https://doi.org/10.1016/0092-8674(92)90029-C

Silver, J., T. Zuo, N. Chaudhary, R. Kumari, P. Tong, S. Giguere, A. Granato, R. Donthula, C. Devereaux, and D.R. Wesemann. 2018. Stochasticity enables BCR-independent germinal center initiation and antibody affinity maturation. *J. Exp. Med.* 215:77–90. https://doi.org/10.1084/jem.20171022

Tiller, T., C.E. Busse, and H. Wardemann. 2009. Cloning and expression of murine Ig genes from single B cells. *J. Immunol. Methods.* 350:183–193. https://doi.org/10.1016/j.jim.2009.08.009

Vale, A.M., J.B. Foote, A. Granato, Y. Zhuang, R.M. Pereira, U.G. Lopes, M. Bellio, P.D. Burrows, H.W. Schroeder Jr., and A. Nobrega. 2012. A rapid and quantitative method for the evaluation of V gene usage, specificities and the clonal size of B cell repertoires. *J. Immunol. Methods.* 376:143–149. https://doi.org/10.1016/j.jim.2011.12.005

Wang, H., and S.H. Clarke. 2003. Evidence for a ligand-mediated positive selection signal in differentiation to a mature B cell. *J. Immunol.* 171:6381–6388. https://doi.org/10.4049/jimmunol.171.12.6381

Wesemann, D.R. 2015. Microbes and B cell development. *Adv. Immunol.* 125:155–178. https://doi.org/10.1016/bs.ai.2014.09.005

Wesemann, D.R., A.J. Portuguese, R.M. Meyers, M.P. Gallagher, K. Cluff-Jones, J.M. Magee, R.A. Panchakshari, S.J. Rodig, T.B. Kepler, and F.W. Alt. 2013. Microbial colonization influences early B-lineage development in the gut lamina propria. *Nature.* 501:112–115. https://doi.org/10.1038/nature12496

Williams, W.B., H.X. Liao, M.A. Moody, T.B. Kepler, S.M. Alam, F. Gao, K. Wiehe, A.M. Trama, K. Jones, R. Zhang, et al. 2015. Diversion of HIV-1 vaccine-induced immunity by gp41-microbiota cross-reactive antibodies. *Science.* 349:aab1253. https://doi.org/10.1126/science.aab1253

Yu, W., H. Nagaoka, M. Jankovic, Z. Misulovin, H. Suh, A. Rolink, F. Melchers, E. Meffre, and M.C. Nussenzweig. 1999. Continued RAG expression in late stages of B cell development and no apparent re-induction after immunization. *Nature.* 400:682–687. https://doi.org/10.1038/23287

Zeng, M.Y., D. Cisalpino, S. Varadarajan, J. Hellman, H.S. Warren, M. Cascalho, N. Inohara, and G. Núñez. 2016. Gut Microbiota-Induced Immunoglobulin G Controls Systemic Infection by Symbiotic Bacteria and Pathogens. *Immunity.* 44:647–658. https://doi.org/10.1016/j.immuni.2016.02.006

Zuccarino-Catania, G.V., S. Sadanand, F.J. Weisel, M.M. Tomayko, H. Meng, S.H. Kleinstein, K.L. Good-Jacobson, and M.J. Shlomchik. 2014. CD80 and PD-L2 define functionally distinct memory B cell subsets that are independent of antibody isotype. *Nat. Immunol.* 15:631–637. https://doi.org/10.1038/ni.2914